AD-778 208

ATMOSPHERIC AEROSOLS BETWEEN 700 AND 3000m ABOVE SEA LEVEL. PART VII. NEW FACILITIES

Reinhold Reiter, et al

Fraunhofer-Gesellschaft

Prepared for:

Army Research and Development Group (Europe)

December 1973

ATMOSPHERIC AEROSOLS BETWEEN 700 AND 3000 m ABOVE SEA LEVEL PART VII

New Facilities

FINAL TECHNICAL REPORT

by

Reinhold Reiter

Walter Carnuth

Hans Joachim Kanter

and

Rudolf Sladkovic

December 1973

EUROPEAN RESEARCH OFFICE
United States Army

Contract Number DAJA 37-72-C-4115

Institut für Atmosphärische Umweltforschung
der Fraunhofer-Gesellschaft

(formaly:
Physikalisch-Bioklimatische Forschungsstelle
der Fraunhofer-Gesellschaft)

D-8100 Garmisch-Partenkirchen
Kreuzeckbahnstraße 19
W-Germany

UNCLASSIFIED
Security Classification

AD 778208

DOCUMENT CONTROL DATA - R & D

(Security classification of title, body of abstract and indexing annotation must be entered when the overall report is classified)

1. ORIGINATING ACTIVITY (Corporate author)
Inst. für Atmosphärische Umweltforschung
81 Garmisch-Partenkirchen
Kreuzeckbahnstrasse 19, West Germany

2a. REPORT SECURITY CLASSIFICATION
Unclassified

2b. GROUP

3. REPORT TITLE
Atmospheric Aerosols between 7000 and 3000 m above Sea Level

4. DESCRIPTIVE NOTES (Type of report and inclusive dates)
Part VII - New Facilities; Final Technical Report

5. AUTHOR(S) (First name, middle initial, last name)
Reinhold Reiter; Walter Carnuth; Hans Joachim Kanter; and Rudolf Sládkowič

6. REPORT DATE	7a. TOTAL NO. OF PAGES	7b. NO. OF REFS
December 1973	97	

8a. CONTRACT OR GRANT NO.	9a. ORIGINATOR'S REPORT NUMBER(S)
DAJA37-72-C-4115	E 1438
b. PROJECT NO. 1T061102B53A	
c.	9b. OTHER REPORT NO(S) (Any other numbers that may be assigned this report)
d.	

10. DISTRIBUTION STATEMENT

Distribution of this report is unlimited.

11. SUPPLEMENTARY NOTES	12. SPONSORING MILITARY ACTIVITY
	US Army R&D Group (Europe) Box 15, FPO N.Y. 09510

13. ABSTRACT

Report details the new laboratory building, apparatus and research facilities which the Institute now occupies. Inclosed are: RAWINDSONDE, High power LIDAR, and an extended computer.

A report setting forth analyses of data will be issued early in the next contract period.

KEYWORDS: (U) Aerosol; boundary layer; exchange coefficient; LIDAR.

DD FORM 1473 REPLACES DD FORM 1473, 1 JAN 66, WHICH IS OBSOLETE FOR ARMY USE.

UNCLASSIFIED

Tabel of contents

ABSTRACT

In the reporting period, a completely new basis was created for our research work in the field of controlling the vertical aerosol structure by meteorological parameters.

1) A new spacious and modernly equipped institute building was moved into which permitted installation and commissioning of the following facilities which were procured and installed in the course of the reporting year:

2) RAWINSONDE for the recording of profiles of temperature, humidity, wind direction and velocity up to about 30 km a.s.l.; balloon take-offs can be freely arranged, depending on meteorological conditions.

3) High-power LIDAR with a pulse intensity of 100 megawatts, sequence of shots up to 1/sec; height of shots up to about 100 km maximum, under favorable conditions.

4) Extended computer with improved data output through fastprint and plot.

Thus work within the reporting period was mainly concerned with installation of old and new facilities in the new building, as well as their commissioning, testing and initial operation. The present report describes facilities and presents and discusses initial measuring examples.

Independent therefrom, the measuring runs of the Zugspitze telemetry system have been continued, evaluated and filed. A detailed scientific analysis will be made in the near future.

Aerosol measurements at our three mountain stations have also been continued and evaluated without interruptions.

Already now, an abundance of interesting relations is found between LIDAR reflex intensity profiles and the directly measured vertical aerosol distributions and aerological data. Systematic comparison programs have been taken up and will be considerably intensified by the EDP system to be procured shortly for connection to the LIDAR.

I. OBJECTIVES AND BACKGROUND OF THIS RESEARCH

The background of our research under Contract DAJA37-72-C-4115 is described in our Final Technical Report (Contract DAJA-37-71-C-3210, Part VI, Chapter I. Besides it is taken to be sufficiently know from earlier reports and publications.

Report Part VI includes the results of the following tasks:

a) Improving the theoretical basis for calculating the vertical profiles of exchange and diffusion coefficient.

b) Obtaining a maximum number of usable telemetry runs throughout the seasons and under varying weather conditions.

c) Classification of data by superordinate aspects, and complete mathematical reprocessing of all data, subsequent to the modification and extension of the comupter programs, and with consideration of (a) above.

d) Derivation of statistically definitely established relations between incremental vertical exchange and diffusion coefficients, on the one hand, and incremental gradients of aerological data, on the other, i.e. parameterization of the relationships for practical application by the meterorologist.

In addition, items a) thru d) have in the meantime been made the subject of a scientific publication, presently being sent to the press.

In the main the following tasks have been compiled as Future Plans in Part VI:

Development of theoretical derivations toward an interpretation of the parametrized functions obtained on the basis of processing all recorded data; fine analysis of the structure of barring layers as well as the development and disintegration of

such layers, influence of time of day, heat absorption, wind and valley circulation etc.; compilation of a statistics of inversions and inversion pattern; inclusion of formation and disintegration of stratus and convection clouds.

However, the following should additionally be essential parts of our future work:
Starting and employment of
a) LIDAR, and
b) RAWINSONDE
with the following objectives:

a) Calibration of the LIDAR system with the aid of the aerosol studies conducted at our 3 stations, and the recordings by the cable cars;

b) Employment of the calibrated LIDAR and the RAWINSONDE in the investigation of aerosol structures and aerosol exchange throughout the troposphere, later to include the area of tropopause and stratosphere; and jet stream investigations.

However, completion of the new institute building, installation of the two units, their gradual commissioning incl. elimination of initial troubles and defects up to the point of "complete readiness" were prerequisite to the employment of the two large-scale units LIDAR and RAWINSONDE.

In view of the considerable amount of time involved in this preliminary work, the latter was given absolute presedence over the theoretical and statistical work listed above under Future Plans. This was an expedient decision also because these latter tasks would have been carried out only with very little effect during the time of moving into the new building and the gradual installation of the computer and its other facilities. For it had become quite obvious that the completion of the new building, and the relocation of the equipment from the old to

the new building plus installation work would take up more of our efforts than had been expected. Another reason was the additional extension of our computer system incident to the move (see III.).

Therefore, this report above all shows the new basis now established for our research work. It describes the new technical facilities and gives examples of their performance and organic interaction within the scope of the extended objectives of our atmospheric research work.

But it must be pointed out that despite the exterior impediment due to the construction of the new institute building and relocation, the recording of all measured values covered by cable car, and their manual and mathematical evaluation as well as their scientific pre-classification were continued with short interruptions only (except for a temporary shutdown of the cable car due to damage caused by an avalanche).

Work on the subjects listed under Future Plans above was just resumed. The results will be presented in subsequent reports.

II. OBTAINING OF DATA

1. Technical Facilities

The facilities described in report Part VI under II.1 remain the same, both at the Zugspitze cable car and at the mountain stations. The telemetry system at the Wank cable car was dismantled.

2. Amount of Processed Data from the Telemetry Systems

Within the reported period, i.e. from 1 July 1972 to 30 June 1973 977 measuring runs by Zugspitze Cable Car System were recorded and evaluated. The recordings were interrupted because of avalanche damages from 10 March to 7 June 1973.

III. DATA PROCESSING

The system of data processing as described in Report Part VI has been retained.

The following components (paid from basic funds) have been added to the electronic computer:

i. Second magnetic tape memory (now a total of two). One magnetic tape each is now separately available for the input and output of data thus considerably facilitating data processing and storing of data.

ii. Fast data printer. It now issues the obtained final results, as far as desired (and not just recorded on tape) in plain language on a wide paper strip. Its printing speed is 100 signs/sec.

iii. A separate computer with 8 k core memory and teletype is now available for solving less intricate problems, testing of programs etc.

iv. Additional staff: An additional physicist with specialized knowledge in mathematics has been hired for solving, in conjunction with the technical staff, all problems within the field of data processing and computer work, and for their execution. He will relieve the physicists and meteorologists of the Institute of that work they up to now had to handle additionally.

It is intended in the course of the following months to also add a television display to the computer system, by which diagrams can directly be made visible very quickly for purposes of checking and fast selection.

Alterations or additions to the computer programs necessitated by the extension of the computer system have been completed.

IV. THE NEW INSTITUTE

1. Location

As section of the 1:50,000 map shows (Fig. 1) the building is located west of the outskirts of Garmisch-Partenkirchen, at a sufficient distance from neighboring building that might in any way interfere with its activities. Fresh air can enter from all sides. A low-grade road passing in a distance of 100 m does not interfere. Telemetry connection with our Zugspitze cable car is effected - as in the past - via a relay station (RS in Fig.1). The relatively low and unobstructed horizon towards WNW and through the open Loisach River Valley towards NNE is essential for radar observations and any further telemetry connections with unmanned stations in the terrain.

2. The Building as a whole

Installation of our special facilities was started in Jan/Feb 1973. The move was carried through in Mar/Apr. The opening ceremony was held on 11 May 1973 with Mrs. Grosholz of the US Army Procurement Agency, Frankfurt/Main, participating as the official representative of the US Army on behalf of the European Research Office, London.

Fig. 2 shows the exterior of the building:

It consists of three floors (basement: shops; ground floor: laboratories and library; top floor: Computer, data processing, and offices; roof: Lidar, radar and all probes), and the attached ballon hangar and garage. It is heated completely by electricity (heating consumption 320 kW; other power consumption 50 kW), and is therefore particularly well heatinsulated against the ambience.

Technical data on the building:

Built-up area:

Main building (13.4 x 34.6 m)	461.9	m^2
Garage and balloon hangar	70.4	m^2
Total space enclosed:	5,824	m^3

Expenses, movable facilities excluded, but heating and all installations included: about 1,8 million DM's

Useful area:

Basement	396	m^2
Ground floor	443	m^2
Top floor	335	m^2
Observation and Lidar/Radar room on the roof	54	m^2
TOTAL	1,228	m^2

Open roof platform for installation of equipment: 360 m^2

3. Roof Platform, floor plan Fig. 3

On the roof platform there is the observation room (2) with LIDAR system (1,1a) and RADAR (1, transmitter/responder on the roof of the observation room).
Others superstructures:
3 - Precipitation measuring equipment; 4 - Meteorological shed for temperatures and humidities, ventilated; 5 - Probes for atmospheric and solar radiations; 6 - Probes for atmospheric electricity and aerosol measurements.

Fig. 4 shows part of the platform; the observation room is seen in the background. It carries radar, masts with probes for wind and atmospheric electricity. Near the left margin: Lidar system, exterior part.

4. Top Floor, floor plan Fig. 5

Description of rooms:

1 - Room for measurements and analog recordings of aerosol sizes, radioactivity and atmospheric electricity, and reception of telemetry signals (also see Figs. 6 and 7).
2 - Computer (also see Fig. 8).
3 - Room with 3 teletypes for the transfer of data to punch tapes.
4 to 15 - Rooms for director, office, and scientific as well as technical staff.

5. Ground Floor, floor plan Fig. 9

1, 2 and 11 - Library and seminar room with service-rooms.
4 - Room for gamma and beta spectrometry (atmospheric radioactivity).
5 and 6 - Physical chemistry lab.
7 and 8 - Chemical lab.
9 - Aerosol lab (also see Fig, 10, instruments for measuring aerosol size distribution).
10 - Physical lab.
12 - Garage
13 - Balloon hangar

6. Basement, floor plan Fig. 11

1 - Pump room (aerosol and radioactivity measurements)
2 to 6 - Store-rooms for raw materials and all kinds of spare parts

7 - Aerosol test room where aerosols of various kinds can be released, also for retention measurements.
10 and 11 - Precision workshops
12 and 13 - Electronic workshops (also see Fig. 12)
14 - Tape store-room
15 and 16 - electric hot-water central heating.

.-.-.-.-.-.

We believe that the above presented survey of our Institute is important for judging the possibilities it offers for the handling of research projects in the field of atmospheric physics and chemistry. Such knowledge is the basis for discussing future research contracts and for the offering of suggestions by our contract partners.

V. RAWINSONDE SYSTEM, FIRST SUCCESSFUL ASCENTS

1. Preliminary Remarks:

As already described in Annual Report VI the setup of an institute-owned Rawinsonde station has been planned with consideration of the following aspects:

1) Parallel measurement of temperature and humidity profiles in free ascent in comparison with the sounding by the Zugspitze telemetry system.

2) Simultaneous recording of the wind profile in the valley up to Zugspitze peak level.

3) Determination of meteorological parameters and making available aerological values required for Lidar measurements above Zugspitze level up to 30 km a.s.l.

2. Description of Equipment Employed

2.1. Type of Sonde:

The VIZ model 1090 sonde (by VIZ Manufacturing Company, Philadelphia) generally employed in the United States was selected for our radiosonde. It consists of a miniature transmitter working on frequency of 1,680 ± 20 MHz. The sonde transmits values of temperature as well as relative humidity as a function of atmospheric pressure. A rod-shaped thermistor (nominal resistance 14 kOhm at 30°C) and a specially coated plastic lamina (nominal resistance 10 kOhm at 33% relative humidity and 25°C) serve as transducers. Dependent on atmospheric pressure a Vidiecapsule moves a switch which alternately connects the two transducers with the circuit of the transmitter. Their change of resistance depending on temperature and relative humidity changes the frequency of an oscillator, thus modulating the carrier frequency of the transmitter. For the purpose of checking the electronic condition of the sonde during flights a reference signal is transmitted at regular intervals in place of relative humidity. The change-over points from temperature to relative humidity of the baroswitch are calibrated by the manufacturer as function of atmospheric pressure, and are furnished in tabular form together with the sonde (Table 1). If respective atmospheric pressure is precisely set before the start, they serve as fixed points for evaluation.

Table 1

2.2. Balloon

The sonde described above represents a payload of about 1,100 g. In order to reach the desired ceiling of 25 to 30 km with this

Tab.1: Pressure Calibration Chart

Contact No.	Pressure	Contact No.	Pressure
1 4 7 -	0 0 0 2 .	0 4 0 -	0 6 0 8 .
1 4 6 -	0 0 0 5 .	0 3 9 -	0 6 1 8 .
1 4 5 +	0 0 0 8 .	0 3 8 -	0 6 2 8 .
1 4 4 -	0 0 1 1 .	0 3 7 -	0 6 3 7 .
1 4 3 -	0 0 1 4 .	0 3 6 -	0 6 4 7 .
1 4 2 -	0 0 1 7 .	0 3 5 -	0 6 5 9 .
1 4 1 -	0 0 2 0 .	0 3 4 -	0 6 6 9 .
1 4 0 +	0 0 2 3 .	0 3 3 -	0 6 8 0 .
1 3 9 -	0 0 2 6 .	0 3 2 -	0 6 9 0 .
1 3 8 -	0 0 2 8 .	0 3 1 -	0 7 0 0 .
1 3 7 -	0 0 3 1 .	0 3 0 +	0 7 1 3 .
1 3 6 -	0 0 3 4 .	0 2 9 -	0 7 2 3 .
1 3 5 +	0 0 3 7 .	0 2 8 -	0 7 3 4 .
1 3 4 -	0 0 4 0 .	0 2 7 -	0 7 4 4 .
1 3 3 -	0 0 4 2 .	0 2 6 -	0 7 5 5 .
1 3 2 -	0 0 4 5 .	0 2 5 -	0 7 6 8 .
1 3 1 -	0 0 4 8 .	0 2 4 -	0 7 7 9 .
1 3 0 +	0 0 5 1 .	0 2 3 -	0 7 9 0 .
1 2 9 -	0 0 5 4 .	0 2 2 -	0 8 0 1 .
1 2 8 -	0 0 5 7 .	0 2 1 -	0 8 1 2 .
1 2 7 -	0 0 5 9 .	0 2 0 -	0 8 2 5 .
1 2 6 -	0 0 6 2 .	0 1 9 -	0 8 3 7 .
1 2 5 -	0 0 6 5 .	0 1 8 -	0 8 4 8 .
1 2 4 -	0 0 6 9 .	0 1 7 -	0 8 5 9 .
1 2 3 -	0 0 7 2 .	0 1 6 -	0 8 7 1 .
1 2 2 -	0 0 7 5 .	0 1 5 -	0 8 8 5 .
1 2 1 -	0 0 7 8 .	0 1 4 -	0 8 9 6 .
1 2 0 +	0 0 8 1 .	0 1 3 -	0 9 0 8 .
	0 0 8 5 .	0 1 2 -	0 9 2 0 .
		0 1 1 -	0 9 3 1 .
		0 1 0 -	0 9 4 6 .
		0 0 9 -	0 9 5 7 .
		0 0 8 -	0 9 7 0 .
		0 0 7 -	0 9 8 2 .
		0 0 6 -	0 9 9 4 .
		0 0 5 -	1 0 0 9 .
		0 0 4 -	1 0 2 1 .
		0 0 3 -	1 0 3 3 .
		0 0 2 -	1 0 4 6 .
		0 0 1 -	1 0 5 9 .
		0 0 0 -	1 0 8 8 .

[redacted]AROSWITCH
[redacted]ERIAL NO:
IS THIS FIRST TIME OF CALIBRATION
[redacted]B. SERIAL NO. -
0-194
[redacted]IZ MANUFACTURING CO.
[redacted]HILADELPHIA PA U.S.A

payload, we selected balloons of 800 g. For these balloons, the supplier (Weather Measure Corporation) claims an average ceiling of 29.5 km.

2.3. Receiver and Tracking Station

The receiver and tracking station is manufactured by Weather Measure Corporation. It consists of individual units functionally arranged; hence is easy to transport and very easy to service. The various units are described below.

2.3.1. Antenna Assembly

The AA consists of a parabolic mirror with a diameter of 1 m. A conical scanning unit and the dipole are located in its focal point. The mirror is flanged on the pedestal of the elevation drive which rests in the fork moved by the azimuth drive. The azimuth drive motor is located in the antenna base. The weight of the antenna reflector is compensated by counterbalance weights.

2.3.2. Antenna Control Unit

The antenna is moved automatically (or by hand) by means of the antenna control unit to follow the motion of the flying Rawinsonde. Due to the conical scanning of the antenna the axis of the lobe of maximum sensitivity rotates on a cone-shaped surface. The sonde is kept in the center of this cone. If the sonde moves out of the center, this will cause a change in amplitude of the received signal. The amplitude variation is converted into error voltages of the elevation and azimuth angles. In case of automatic follow-up these error voltages are used to control the synchro-servo-system effecting the follow-up. The antenna continues to be moved until the error voltages are balanced to zero. In case of manual follow-up this balancing is to be accomplished

by the operator by means of two handwheels. If automatically operated the follow-up speed amounts to 5 degrees per second; if manually operated 10 degrees per second. A decoder transfers the angular setting of the antenna to the digital printer described below.

2.3.3. Receiver

The sonde signal received by the antenna is transferred to the receiver. An internal oscillator generates a signal of 1,650 MHz, about 30 MHz lower than the sonde signal. Both signals are transferred to a mixer. In the i.f. amplifier the 30 MHz output of the mixer is split into an amplitude-modulated and a frequency-modulated component. The former is transferred to the antenna follow-up control (see above). Decoding of the frequency-modulated signal yields an audiosignal ranging from 8 to 200 MHz which, after demodulation, is transferred to a recorder for recording of temperature and humidity values. Before the start the receiver must be tuned in with the respective transmitter frequency.

2.3.4. Data Output

a) The Digital Printer

The angle values of elevation and of azimuth as functions of time, which are transferred from the antenna control, are printed out by the digital printer according to the following pattern:

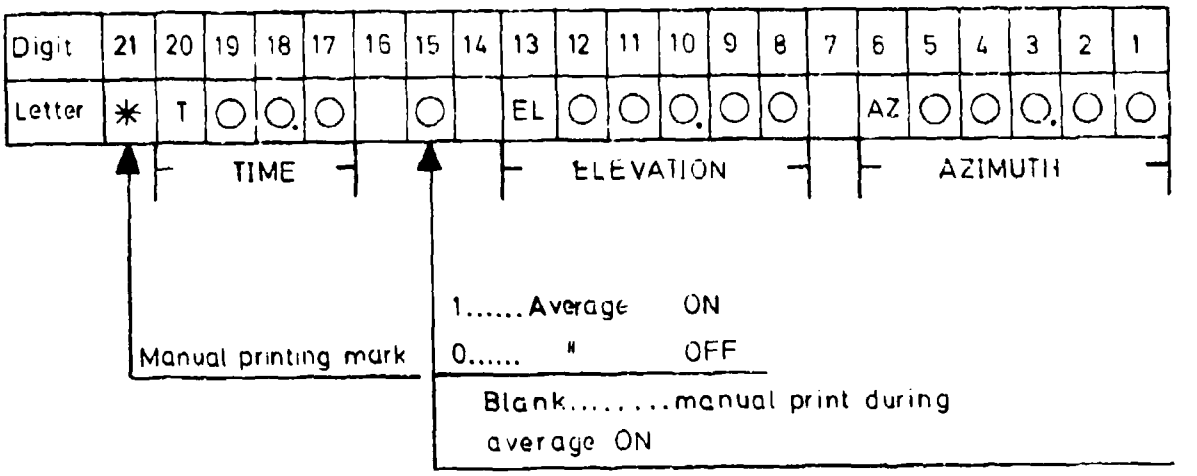

Table 2 shows a print-out example.

Tab.2 : Print of Elevation and Azimuth

	T4[illegible]	1	EL02[illegible]	AZ15[illegible]7
	T390	1	EL0216.37	AZ155.46
	T380	1	EL0226.39	AZ156.680
	T370	1	EL0236.69	AZ159.18
	T360	1	EL0246.46	AZ159.38
	T350	1	EL0246.91	AZ1606.78
	T340	1	EL0256.18	AZ1626.39
	T330	1	EL0266.12	AZ1654.10
	T320	1	EL0276.78	AZ1656.77
	T310	1	EL0286.72	AZ1676.42
	T300	1	EL0296.20	AZ1[illegible]6.07
	T290	1	EL0296.83	AZ1706.58
	T280	1	EL0316.01	AZ1726.14
	T270	1	EL0316.69	AZ1736.27
	T260	1	EL0316.75	AZ1744.27
	T250	1	EL0306.65	AZ1766.31
	T240	1	EL0296.81	AZ1786.30
	T230	1	EL0296.34	AZ1806.08
	T220	1	EL0286.84	AZ1816.65
	T210	1	EL0286.37	AZ1846.23
	T200	1	EL0256.49	AZ1876.49
	T190	1	EL0256.96	AZ1906.67
	T180	1	EL0256.66	AZ1946.24
	T170	1	EL0236.92	AZ1986.09
	T160	1	EL0226.73	AZ2026.21
	T150	1	EL0226.44	AZ2066.09
	T140	1	EL0216.53	AZ2096.46
	T130	1	EL0196.99	AZ2136.38
	T120	1	EL0186.45	AZ2176.29
	T110	1	EL0176.42	AZ2206.91
	T100	1	EL0166.01	AZ2246.21
	T090	1	EL0146.11	AZ2276.83
	T080	1	EL0116.79	AZ2306.19
	T070	1	EL0096.50	AZ2336.22
	T060	1	EL0056.78	AZ2366.05
	T050	1	EL0036.36	AZ2386.04
	T040	1	EL0016.01	AZ2396.19
	T030	1	EL3586.69	AZ2386.76
	T020	1	EL3566.10	AZ2386.13
	T010	1	EL3536.61	AZ2386.01
R	T000	0	EL3526.19	AZ[illegible]6.06

	T100	1	EL0226.63	AZ1206.99
	T090	1	EL0236.14	AZ1216.40
	T080	1	EL0256.97	AZ1216.58
B	T070	1	EL0286.36	AZ1216.50
	T060	1	EL0286.33	AZ1216.96
	T050	1	EL0286.35	AZ1226.15
	T040	1	EL0286.38	AZ1236.40
	T030	1	EL0286.30	AZ1266.78
	T020	1	EL0286.42	AZ1286.21
	T010	1	EL0286.34	AZ1296.92
	T000	1	EL0286.37	AZ1306.56
	T990	1	EL0286.21	AZ1256.41
	T980	1	EL0286.08	AZ1256.97
	T970	1	EL0276.95	AZ1266.25
	T960	1	EL0276.76	AZ1266.69
	T950	1	EL0276.81	AZ1276.18
	T940	1	EL0276.74	AZ1276.95
	T930	1	EL0276.64	AZ1286.56
	T920	1	EL0276.52	AZ1296.15
	T910	1	EL0276.44	AZ1296.43
	T900	1	EL0276.33	AZ1306.62
	T890	1	EL0276.23	AZ1296.58
	T880	1	EL0276.05	AZ1296.86
	T870	1	EL0266.78	AZ1296.98
	T860	1	EL0256.38	AZ1306.17
	T850	1	EL0256.80	AZ1306.51
	T840	1	EL0256.34	AZ1306.45
	T830	1	EL0246.95	AZ1306.58
	T820	1	EL0246.79	AZ1306.72
	T810	1	EL0246.82	AZ1316.02
	T800	1	EL0246.63	AZ1316.31
	T790	1	EL0246.32	AZ1316.45
	T780	1	EL0246.24	AZ1316.59
	T770	1	EL0246.04	AZ1316.69
	T760	1	EL0236.97	AZ1316.72
	T750	1	EL0246.11	AZ1326.19
	T740	1	EL0236.97	AZ1326.58
	T730	1	EL0236.80	AZ1326.86
	T720	1	EL0236.59	AZ1336.07
	T710	1	EL0236.33	AZ1336.55
	T700	1	EL0226.69	AZ1346.21

R : Balloon Release

B : Balloon Burst

Print-out frequency is selectable between 10 times, twice, and once per minute.

With automatic tracking the values are printed out in black, with manual tracking in red. Manually interrogated intermediate values are additionally marked by an asterisk. Negative elevation angles - in our case an observing of the sonde from the valley below Wank peak level - are put out as angles complementary to 360°. A built-in miniature computer, upon interrogation, puts out the arithmetic means of the angles over one minute each time.

b) Output of Values of Temperature and Humidity.

The recorder used for this purpose is a single-channel continuous recorder. Temperature and humidity values are alternately recorded, by scale divisions (1 scale division corresponding to 1% of full-scale deflection), as functions of time (exact paper feed 20 mm per minute). By the calibration scale coming with the radiosonde each change-over point from temperature to humidity recording designates a defined value of atmospheric pressure. Thus the time scale is directly correlated to the pressure scale; example: ascent of 10. August 1973, Fig. 13.

3. Placement of Equipment

3.1. Receiving Station

The receiving station was installed in our mountain observatory on Wank peak (1,780 m a.s.l., approximately 1,000 m above the valley floor). The antenna is mounted on a self-supporting steel mast of about 4 m height (cf. our Annual Report VI) at the level of the measuring platform of the observatory. It is protected against icing and other weather effects by a heated radome (Fig.14)

Reiver, antenna follow-up and data output are located in the main room of the observatory (Fig. 15).

3.2. Take-off Site

The balloon take-off site is located right next to the Institute building (735 m a.s.l.). It was found that even with weak surface winds, take-off is possible immediately in front of the hangar, whereas in strong-wind situations it is intended to shift over to an adjacent meadow.

Preparing the balloon for flight is done inside the hangar (Fig. 16). Because of the great danger of explosion of the hydrogen gas used for filling, all electrical devices are of the explosion-proof type. To prevent mechanical damage to the balloon, an interception net is spread out at a distance of 0.5 m below the hangar ceiling. The filling apparatus is located at a table of 3 m^2. Prior to filling, the balloon is spread on this table. To keep friction low between balloon and table, the latter is powdered with talc. Cotton gloves are worn for all manipulations on the balloon to prevent the placing of grease traces on the outer skin of the balloon.

Preparation of the sonde is done on the apron in front of the hangar. A modified thermometer hut is used for calibrating the sensors for temperature and humidity. This hut contains a psychrometer which can be read from outside and which is ventilated by an aspirator located outside the hut (Fig.17).

4. Performance of a Flight

If the weather maps received via a facsimile reiter indicate that a weather condition of interest to our specific investigations is developing for our area, one or several flights are set on short notice. For this purpose our Wank peak antenna

station is manned with an additional operator. Preparations at the take-off site are conducted by two men. Antenna and take-off are in speech communication by means of powerful radio sets.

To begin with the antenna system is started up and checked out for operability by means of checklist. This check encompasses all electrical and mechanical functions of the antenna system.

Meanwhile the balloon is prepared for filling at the take-off site, the humidity sensor inserted in the sonde, and the battery prepared for activation. All essential data such as sonde number, actual near-ground weather and atmospheric pressure are recorded. The ropes needed for the balloon train are readied and the parachute is unfolded. Then the battery is activated by two minutes of watering, and after draining is inserted in the sonde. Thus the transmitter is activitated.

Now the receiver is tuned to the transmitter frequency of the sonde, which as stated above may deviate by 20 MHz from the 1,680 MHz nominal frequency. For the subsequent tests the sonde is inserted in the calibration hut, and the latter closed for proper air conditioning.

The sonde has test connections for a manually operated switch so the signal transferred can be varied externally, bypassing the baroswith.

When the receiber is tuned, a refernce signal is transmitted at first. This serves to calibrate the recording amplitude of the temperature/humidity recorder (95% of full scale). Then the temperature sensor and the humidity sensor are activated successively and their values recorded over a period of sufficient lenght. Simultaneously the values of the psychrometer

which can be read through a window of the calibration hut, are noted down. These values along with the recordings of the recorder represent the base-line check of temperature and humidity for later evaluation (see below).

Next, the sonde is removed from the calibration hut and the baroswitch set to actual barometric pressure (Fig. 18). This setting can be done in increments of 0.5 mb. Pressure setting completed, the sonde is ready for take-off.

During calibration the ballon is filled (filling time about 15 minutes, cf. Fig. 19). The filling socket is constructed as a weight dimensioned to compensate the weight of the sonde and the necessary free lift. A free lifting power of 1 kp was selected conferring upon the ballon a mean rate of climb of 200 m per minute.

After the balloon is filled the train is set up (Fig. 20). The distance from the balloon to the parachute is about 2 m, that from the parachute to the sonde about 25 m. Thus the overall lenght of the balloon and sonde train is about 32 m. This lenght is necessary to prevent vitiation of the measured values by the flow field around the balloon.

Take-off is accomplished by countdown via radiotelephone, so as to synchronize take-off and tracking.

5. Evaluation

5.1. Evaluation of Temperature and Humidity

For the time being, temperature and humidity recordings are evaluated as follows:

First, the scale sections pertaining to the pressure dependent switch-over points from temperature to relative humidity are transcribed into tables, and the appertaining times relative to take-off are determined by the paper feed. With special slide rules, the readings are converted into temperature and relative humidity values, considering calibration. Relative humidity is additionally transformed into dew point differences. These values are entered into a Stuewe type graph for further processing.

5.2. Wind Evaluation

Wind values are available digitally as a funtion of time in the form of elevation and azimuth angles. From the temperature/ pressure curve the altitude of balloon position is calculated by computer for the respective point of time, using the barometric formula for altitude. From altitude and elevation angle the horizontal distance of the balloon from the point of observation is calculated by an appropriate computer program, and from the change of this distance between two consecutive times along with the change of the respective azimuth, mean wind velocity and direction are calculated for the layer that was traversed by the balloon in the associated time. From these values the trajectory of the balloon flight and the wind profile can be plotted. This evaluation work is done by computer.

6. Initial Experiences

6.1. General

A total of 5 ascents were conducted to test the system. All instruments involved as well as organization of the flights have fully stood the test.

The following heights were reached: 16,32,25,13 and 23 mb,

which means that all balloons except one have reached the required height of 25 km. The maximum height reached was 29.8 km.

In all cases it was possible to turn on automatic tracking shortly after take-off, while the balloons were still inside the valley below Wank peak level. No problems were experienced in handling the instruments. Even after balloon burst it was possible to record the values of the sonde descending on its parachute till the sondes dropped below the horizon.

6.2. Analyzability of Data

6.2.1. Temperature and Humidity

a) Comparing Ascent of Sonde against Descent

With all flights, recordings of temperature and humidity were capable of being evaluated right from take-off. The attempt was made to also evaluate the values of the sonde descending on its parachute. No problems were experienced (Fig.21). This result is of particular interest inasmuch as from one flight two soundings can be obtained in this manner. This is considered of particular importance in case of any northern conditions. The balloon would then ascend within dynamic air pressure and go over the main range of the Alps. Temperature stratification on the lee side, i.e. within foehn, could then be studied by the descending sonde.

b) Comparing Balloon Sonde against Cable Car

Soundings between valley level and Zugspitze peak level by balloon sonde were compared with simultaneous soundings by cable car. This revealed systematic deviations of temperature

values (Fig. 22), relative to the entire height interval (about 2,000 m). It is assumed that the cabin in some way exercises an effect on the cable car sensors. Such sources of error can now be studied and eliminated through the possibility of comparison offered by the radiosonde. The error now discovered is, however, of no influence on previous evaluations of cable car soundings because we were operating only with gradients across very small height intervals. In this case the deviations are to be neglected.

c) Comparison against Radiosonde Ascents of Munich and Stuttgart

Comparing one ascent of 31 August 1973 with simultaneous Munich and Stuttgart radiosonde ascents (Fig. 23) reveals considerable conformity in temperature profile with the Munich ascent. Distinct variations are, however, found already in the humidity profile. The humidity profile obtained by our ascent is between that of Munich and that of Stuttgart, revealing variations caused by differing orography and special distance (distance between Munich and Garmisch-Partenkirchen is about 80 km). In evaluating the data of our sonde it is intended to always include the Munich and Stuttgart ascents, maybe also those of Payerne and Prague. In northern conditions which are of interest to us, this will permit conclusions as to cyclonic and anticyclonic effects in conjunction with the jet-stream from northern to southern direction.

Moreover, our sonde offers the advantage of time-independent ascents at optimum time for our measurements. In addition our ascents are evaluated in all fine details up to bursting height of 25 to 30 km, and thus offer considerably more detailed information than the routine ascents of the weather services which include values of the main pressure surfaces and of the distinct points only.

6.2.2. Wind Evaluation

It was shown that wind evaluations from inside the valley are not possible. Obviously, the sonde signals are so much interfered with by reflexes from precipices that the angle of elevation necessary for calculating horizontal distance cannot be measured with sufficient accuracy. Besides, this angle is very small for station points of the sonde from the valley, hence even minor inaccuracies in determining the angle enter very effectively into the calculation.

Acceptable wind evaluations were always found from 2,500 m on. Attached Figures 24 and25 show two examples. In their upper part the figures plot the trajectory of the balloon flight; in their bottom part the measured wind profile in velocity (left side) and direction (right side).

On 16 August 1973 the station was in a weak east current at the southern margin of an anticyclonic area extending from Northern Italy to Scandinavia. The current extends up to a height of 12 km. Wind maximum is at about 9 km. Above 12 km the wind quickly shifts to North. Shifting winds are observed in the stratum up to 18 km. Above, an eastern condition is again found (Fig. 24).

On 31 August 1973 typical rear weather prevails in our area. On the preceding day polar air had advanced to the Mediterranean and led to the formation of a Genova cyclone. On 31 August 1973 our station is in a cool, rainy weather.

The wind profile (Fig. 25)in this case is particularly instructive.Wind from North-West/North is observed up to 4 km. Above, the wind rapidly shifts via North to South/South-West. This shows clearly that our station is still on the front of the high-level trough belonging to the cold-air advance. Wind maximum is reached at 10 km, right below tropopause level

(about 11 km). Shifting winds prevail at tropopause altitude. Above, the wind shifts to West/North-West. Above 20 km, direction of wind varies very much.

6.3. Summary

Summing up it can be said that the Rawinsonde system meets all requirements demanded of it. Directed to specific objectives it supplements all programs being pursued. Conceptions developed thus far on microscale and large-scale exchange processes can be checked and individual aspects verified. Besides, the RAWINSONDE data form the basis for aerological evaluation of the LIDAR reflex intensity profiles between 2,500 m and 30 km a.s.l..

VI. DESCRIPTION OF LIDAR SYSTEM; INITIAL EXPERIENCE AND RESULTS

Basically the Lidar system consists of the following four main components (see general-view photograph. Fig. 26):

1) laser head (a) with fluorescence suppression and trigger sensor (b);

2) operating desk (c) containing the necessary auxiliary units (cooling system for laser, multiplier cooling, and voltage supply for PM (PM = photomultiplier)), and upon which t^2-control (d), oscilloscope (e), adjusting device (f), and operating console (i) are mounted. The laser head (a) is mounted on the frame of the desk structure.

3) power pack with control electronics for Q-switch operation (g);

4) receiver with Cassegrain reflecting telescope, PM in cooling, box, filter, diaphragms, neutral wedge, adjusting device, heating, etc., all of which are installed outside.

The following is a detailed description of the main components and their functions:

1. Laser Transmitter (Fig. 26)

The laser operates on a Czochralski type ruby of choice quality, about 165 mm long, diameter: 9,5 mm, end faces coated. The ruby is located in a solid case, more specifically in a cavity of the latter, having a cylindric-elliptical cross section, lined with mirror-finished solid silver. The pumping flash lamp (Type FX 47-C 6.5 of EG and G) is also installed in said cavity. For protection as well as for cooling-water conduction, the ruby and flash lamp are enclosed in quartz glass tubes. For keeping the ruby end faces clean, and espicially free of condensed water and dust, dried and filtered air from our Institute-owned compressed-air line is blown on the end faces (Fig. 26 b).

The laser resonator consists of a dielectric mirror having a reflectance of 99.7% for the ruby wavelength of 6943 angstroms, plus a BK-7 glass plate with a reflectance of 16% as an output mirror. In order to produce laser pulses of the highest possible performance and of short duration, a Q-switch device is provided. Without it the ruby laser would emit a pulse of approxmantely 1 msec duration consisting of a great number of individual peaks (spikes), which would be useless for the intended purpose. By means of Q-switch, on the other hand, one single, very energetic so-called giant pulse is obtained, provided care is taken to ensure that the optical resonator does not become oscillatory until the ruby has built up its maximum degree of inversion, which is the case after approx. 1 msec. This is achieved by a suitable optical switch placed in the beam path within the resonator, reducing the Q-factor of the resonator to a point where no laser oscillations can

arise. The following are used for this purpose: mechanical choppers (rotary sector diaphragms); absorbing, saturable dye cells; and electronic switches consisting of polarizers and optically active, electrically controllable elements (Kerr or Pockels cells) which become optically active upon application of an electric field. This latter method constitutes the most expensive solution, but the most elegant and most reliable, too. Unlike the Kerr cell, which is filled with poisonous nitrobenzene which needs to be replaced every so often, the Pockels cell operates with a crystal (e.g. KH_2PO_4) as its optically active medium. Hence it is maintemance-free and more convenient to handle. Its disadvantage is that the electric field must be applied longitudinally, that is parallel to the beam path, hence the electrodes need to be perforated and, as a result, field distribution within the cell is not quite homogeneous. Consequently, the Pockels cell is not opened evenly throughout its cross section. This disadvantage is of particular consequence when maximum power is required. By contrast, the Kerr cell with which the field is applied transversly will open evenly throughout its cross section.

With both the Kerr and the Pockels cell two modes of operation are available, that is with bias voltage or with pulse drive. In the latter case, the cell and polarizers are arranged so that in electrically dead condition the optical path is blocked, and vice versa. With a Kerr cell the mode of operation based on bias voltage is more advantageous since with the electric field applied constantly any impurities in the nitrobenzene will migrate to the electrodes. In addition, shorter switching periods are realized in this manner.

With our unit both the Kerr and the Pockels cell were optionally provided for. At the time of delivery, a Pockels cell with pulse drive and requisite control electronics (cf. part VI.3) as used by other research teams was installed. In agree-

ment with the manufacturer, a Kerr cell with bias voltage was later installed to take advantage of its superior switching properties. This noticeably improved the efficiency of the laser. We were able to achieve the same laser pulse power with almost 20% less flash-lamp power.

This conversion necessitated replacing the control electronics intended for the Pockels cell by a Kerr driver (for details see part VI.3). This, however, led to the consequences regarding fluorescence suppression described below.

1.2. Fluorescence Suppression

In addition to the laser light the ruby also emits incoherent fluorescent light. Although the latter is divergent and of very low intensity in comparison with the laser pulse, nevertheless, with the weak reflected signals to be received from great altitudes, this fluorescence would under unfavorable conditions introduce into the receiver so much reflected light from nearby as to be in the same order of magnitude as the wanted signal. In order to keep this fluorescent light from the laser exit, fluorescence suppression is provided. At time of delivery of the system an arrangement was provided for eliminating the nonpolarized fluorescent light. It consisted of two polarizers and one Kerr or Pockels cell, which was blocked in the inactive state and activated along with the Q-switch. It can be installed inside or outside the laser resonator. Both arrangements involve considerable disadvantages. The additional glass air surfaces, which cannot be coated of the high-power density, cause a considerable loss in efficiency. If the arrangement is installed outside the resonator this involves a decrease in transmitter output power since, for stability reasons, laser power cannot be further increased. Also, because the resonator must be shortened, the natural divergence of the beam is increased. If the fluorescence suppression is

located inside the resonator, the loss of light can be compensated by increasing the flash-lamp pump power, however, that would be at the expense of the life to the lamp. In addition, adjusting this arrangement is extremely difficult.

Due to the replacement of the Pockels cell in the Q-switch by a Kerr cell with bias voltage we encountered a different situation since it is impossible in this case to operate the Q-switch and the fluorescence suppression simultaneously with just one control unit. The Kerr driver produced in quantity by the manufacturer is designed only for the $\lambda/4$ voltage which with our Kerr cell is at 16 kV and causes a rotation of the direction of polarization by 45°. Since in the Q-switch the light passes through the cell twice, this is sufficient to block the light path. In the fluorescence suppression, however, the beam passes through the cell just once and therefore must be rotated in its direction of polarization by 90°. This would require a bias voltage of 23 kV ($\lambda/2$ voltage) for which the Kerr driver is not designed. We therefore decided to replace the active, electronically controlled fluorescence suppression by a passive cell filled with a saturable absorber (crypto cyanine). Such cells can also be used as Q-switches.

In such cases, where the cell is to block the normal laser pulse, adherance to the optimum dye concentration is very important as the saturation threshold is dependent thereon. By contrast, dye concentration is much less crucial in the case of ruby fluorescence suppression. The dye cell has the advantage of having just two glass air surfaces and therefore involves much less loss of light than the arrangement originally provided. It can be mounted outside the resonator without the latter having to be shortened, and can be quickly removed when not needed. The effort involved in the occasional replacement of the dye solution can be put up with, especially as a fully equipped chemical lab is available at the Institute.

Finally, it is not yet definitely certain whether fluorescence suppression will be needed at all in view of the very favorable climatic conditions prevailing at the site where e.g. ground fog is extremely rare.

1.3. Trigger Sensor (Fig. 26 b)

The small amount of laser light passing through the 99,7% reflectance dielectric mirror is used for triggering the oscilloscope. Through a diffusion screen it falls upon a fast photodiode whose output signal is converted by a connected, battery-operated pulse shaper stage into a unit pulse of 20 V height. The latter starts the X-time-base generator of the oscilloscope via the later's external trigger input. It also triggers the t^2-control which will be described below.

2. Operating Desk (Fig. 26 c)

The operating desk on its frame structure supports the laser head. It further serves for mounting the following auxiliary devices and accessory units.

2.1. Cooling System for Laser

By changing 5 cocks the laser can optionally be cooled directly by tap water, or indirectly by a secondary circulation. Indirect cooling was provided to keep dirt deposition in the laser head low. From a storage container the cooling water is pumped through a heat exchanger wherein tap water is circulating, then through a filter, and an air cushion for absorption of vibration, into the laser head, and subsequently back into the container. A protection switch in the secondary circulation will cut out the water pump (and thus interrupt

the interlock system, too; cf. Part VI.3), if the cooling water becomes too warm (switch point is adjustable), or the rate of circulation too low.

The possibility of direct cooling had been provided to ensure the greatest possible pulse repetition rate at full load as it was supposed to be mor effective than indirect cooling. In the final result, however, it is less effective due to the low water pressure of about 2 atmospheres absolute pressure available on the top floor of our Institute building. Particularly if air gets into the laser head, e.g. after disassembly, air bubbles are retained inside the cavities for an extended period of time, impairing the focusing of the flash-lamp light and thus further reducing efficiency.

After extended operation with indirect cooling, however, the formation of a dark, reddish deposition was found on the flash lamp and the reflector, again considerably reducing output. It is assumed these are components of the PVC tubing which gradually accumulate in the secondary cooling water and are decomposed by tne intensive light of the flash lamp. This phenomenon does not occur if the secondary cooling water is renewed at regular intervals.

2.2. Multiplier Supply with t^2-Control (Fig. 26 d)

The operating voltage for the photomultiplier (800 to 1800 V, depending on background luminosity) is supplied by a highly stabilized Ortec high-voltage unit. The t^2-control serves the purpose of making the returned signal independent of range, for a certain range interval, by compensating for the usual inverse square losses. This means that amplification of the receiver must increase by the square of running time t counting from the moment of the Q-switch on. This

could be accomplished e.g. in a succeeding amplifier having a variable amplification factor. In our system, the sensitivity of the PM itself is controlled which provides the additional advantage of reduced overload by the intense short-distance signal. Direct control of the PM amplifier via the voltage of the dynodes is unsatisfactory since the drive signal would act as an interference in the measuring signal at the outlet due to the capacitive coupling of the dynodes. For this reason, control was applied, for the first time in the case in question, by deflecting the electron flow from the dynodes within the PM by means of an electromagnet, and thus controlling amplification.

The current in the deflection coil varies with time in such a manner that the Photomultiplier amplification varies in proportion to the square of time. The t^2-control works as follows (see block diagram Fig. 27):

A positve reference pulse generated at the power pack in conjunction with the ignition of the flash lamp (see part VI.3) starts a function generator which generates a linearly increasing voltage. The negative pulse, supplied by the trigger sensor at the moment the laser beam leaves the transmitter, stops this increase and effects a linear drop of the voltage of the function generator (if this pulse is not produced, a security circuit will produce a corresponding pulse, after 2 to 3 msec, which effects the linear drop). A limiter unit ensures that the voltage will not exceed certain maximum values. A stabilizing circuit prevents drifting of the quiescent current from its neutral position. A power amplifier passes the signal of the function generator into the control coil of the PM. Within this circuit there is a measuring resistor whose voltage drop is required for the negative feedback of the power amplifier. This negative feedback produces the proper time variation of the coil current.
It is basically consists of a series of potentiometers by

which the desired control path is generated element by element, via succeeding amplifiers. The negative feedback can to a very great extent be adapted to the desired curves. In particular, powers of t other than 2 would be possible.

Inasmuch as the dynamic range of the PM is not unlimited, the t^2-control covers an amplification range of no more than 2.5 powers of ten. Consequently the running time of the control is limited to the range of 13.3. to 266 µs corresponding to a height interval between 2 and 40 km (although it is still possible to shift it). Above and below this range, PM amplification remains constant.

In operating the t^2-control one must remember that the background signal, which is normally constant, will increase along with t^2, and superimpose itself upon the measuring signal. Furthermore it must be borne in mind that due to the limited continuous-current rating of the PM practically no signal is to be expected, during daytime, from the lowermost 2 km of height. For this reason use of the t^2-control is advisable only in the nighttime.

2.3. Multiplier Cooling System

The control unit for the PM cooling is also installed in the bench. Detailed description of the cooling system as such and its functioning is found in the paragraph on the receiver system.

2.4. Oscilloscope (Fig. 26 e)

For displaying the measuring signal as a function of travel time, we use a 50 MHz oscilloscope Tectronix model 556. This is a genuine double-beam oscilloscope with two completely

separated cathodes, deflecting systems, and X- and Y-amplifier. Therefore, the vertical and the horizontal time-base velocities may be set independently. In addition it is possible to have the second system triggered by the first one, with a time delay which may be precisely set. This device may be used to advantage in displaying part of the measuring signal, extended in time and with increased resolution. That portion of the signal which is covered by the second system can be identified by increased brightness on the curve of the first system. A model C-27 Tectronix oscilloscope camera with a lens aperture of 1:1.3 and an object-to-image ratio of 1:0.5 is used for image photography. In addition to a Polaroid roll film back, a camera back is available for normal perforated 70 mm film. The Polaroid process offers the advantage that the picture is ready a few seconds after exposure and can be repeated immediately, if required. However, this is very expensive in operation. On the other hand, normal film material is less costly and can be utilized better in that the picture is then available in the form of a transparent negative which may be projected or enlarged more easily. For this purpose a conventional enlarger is available.

2.5. Adjusting Device (Fig. 26 f)

For adjusting our laser resonator we use a 2 mW He-Ne gas laser which is mounted perpendicular to the beam direction, on an adjustable support sitting on a sturdy lateral arm. The gas laser beam is directed into the resonator of the ruby laser by a divider cube which is also adjustable. Thanks to this stable mounting the He-Ne-laser can stay in place, marking it possible at any time, such as after a necessary cleaning of the laser head, to quickly readjust the ruby laser.

3. Power Pack (Fig. 26 g)

The power-pack support frame contains the power supply and the ignition device for the flash lamp plus the electronic control device for the Q-switch, whose functions are described below.

3.1. Power and Ignition Unit

The functioning of the power pack proper is detailed by the symbolic circuit, Fig. 28. Power is fed from the 3-phase mains into the charging circuit (upper left) via three 35 amp fuses and the main switch. A 3-phase transformer supplies the necessary high voltage which may be rectified and, via ignitron V_2, fed to the working capacitors in the buffer and discharging circuit. The ignitron consists of spark tube which, similar to a thyratron, is started up by a pulse, and then will stay conductive as long as a certain minimum voltage is applied to the anode.

The voltage on the capacitors (a total of 782 mfd) is collected via a chain of resistors, conducted through an indicator, and applied to voltage control. This action, in detail, is as follows: The charging voltage is set digitally on a helipot in the front panel. If actual voltage is considerably below required voltage, the required-actual comparator will issue a pulse via the b-outlet. For safety reasons, on initial switching-on of the power pack, this pulse is delayed by 2 seconds, otherwise by 20 msec, and then, via a pulse amplifier with shaper, starts up the V 2 ignitron so the current may flow from the charging circuit into the storage capacitors. As soon as the required value is reached, the required-actual comparator, via its c-outlet, issues a pulse to the cutoff stage control which, via the d-line, arrives in

the pulse amplifier with shaper, and by the V 1 cutout ignitron cuts out the V 2 ignitron. These actions proceed so fast that in each instance the final voltage is maintained to within 1 %.

As soon as the capacitor is charged, but is not discharged, slow discharging occurs in the storage capacitors due to unavoidable leakage resistances. To make up for the loss, in case of slight deviations from the required voltage, the required-actual comparator will issue a signal to the recharge control causing the losses to be balanced out.

The discharge of the working capacitors into the laser head is initiated by the trigger unit. Simultaneously, the latter issues striking pulses to the V 3 ignitron and the ignition unit of flash lamp V 5. Normally it would not be necessary for the V 3 ignitron to be in this line. It was additionally incorporated to prevent the charging voltage from being constantly applied to the flash lamp. Thus it is possible to cool the laser head with ordinary tap water without the risk of electrolytic phenomena occuring. The flash lamp cannot ignite on the working voltage alone; it requires an additional striking pulse of about 30 kV. The latter is generated in the ignition unit by the capacitor (wich is connected in series with the primary winding of the transformer) being ignited via the V 5 spark lamp. Choke Ch 2 located between ignitron and striking-pulse transformer in the ignition unit serves to lengthen the pulses, at the same time decreasing the peaks and thus sparing the flash lamp.

All three switch tubes within the discharging circuit are started up by the trigger unit via the appropriate pulse amplifiers. The triggering as such may be actuated by one of several actions: by a positive pulse, or by closing of a circuit, the pulse-shaping stage will generate a pulse which is

sent, via a pulse counter, to the three pulse amplifier stages, and will trigger the discharge of the storage capacitors into the flash lamp. Besides the closing of the circuit or a positive pulse, triggering can also be actuated by an internal frequency generator (not shown in Fig. 28) which is continuously variable between 0.1. Hz and 2 Hz. By a relay the output pulses are issued to the shaper. This permits a changeover from individual pulses to frequency generator or vice versa by remote control also.

Simultaneously with the ignition of discharging tube V 3, the appropriate pulse amplifier will issue a reference pulse of 10 V which is used to start up the Q-switch driver (see below). For the rejection of any discharge overshoots an additional ignitron V 4 is provided which is turned on by the undesired overshoot and permits faster recharging, at a lower load on the power supply. Overall, the power pack is so well engineered that it imposes no limitation on laser performance, either in pulse power or in pulse repetition frequency.

Because a certain danger factor is presented by the high charging voltage, an interlock system is incorporated which will prevent actuation of high voltage or immediately discharge the capacitors, in the event of several improper circumstances. For example, if cables are not correctly connected, or if the cooling water pump is not running, then the interlock system will immediately discharge the storage capacitors. Basically it consists of a number of switches connected in series, which are placed at the respective locations (e.g. at the bushing for the power cable to the laser head). As soon as just one of these switches is open one circuit is cut out, and charging of the reservoir capacitors is blocked via a number of relays. A "GO"-lamp will go on as soon as the interlock circuit is closed. Originally the necessary electronic

device for operating the Pockels cell had been installed in the power-pack support frame, as is apparent from Fig. 26. It consisted of a trigger delay generator or retarder issuing a pulse after an adjustable time subsequent to the reference pulse coming from the discharging circuit, plus a trigger power amplifier which issued a delayed high-power pulse to the Pockels cell by capacitor discharge via a hydrogen thyratron. For operating with a Kerr cell with bias, the two aforementioned plug-in units were replaced by a Kerr driver (provisionally placed on top of the power pack in Fig. 26).

The Kerr driver contains a high-voltage generator, adjustable up to 20 kV and a delay unit. The Kerr cell is connected to the high-voltage via a triggerable spark gap. Shortly after actuating the high voltage, a residual current of several hundred μA, more or less sharply decreasing depending on the aging state of the Kerr liquid, will flow through the Kerr cell, especially if it has not been in operatin for some time; this current may be read off an instrument. After several minutes this residual current will reach a stationary value of about 5 up to 30 μA depending on condition of liquid. The input of the delay unit is wired to the reference pulse output of the discharge circuit. At an adjustable time interval after flash lamp ignition the spark gap is triggered via another pulse line; the voltage on the Kerr cell will collapse within a very short time, the laser resonator is started up, and the Q-switch pulse is initiated.

4. Receiver Unit

The receiver unit whose individual parts are described in detail below, is installed in a vertical, barrel-shaped waterproof case permanently mounted in the open on the observation platform. The unit is mounted for vertical firings only for

reasons of cost as well as of safety because of the mountainous surroundings. The receiver unit consists of following components:

4.1. Receiver Case

The barrel-shaped case is closed on top by a tilted plate-glass pane allowing the rain or snow water to flow off easily, with the transmitter exit window placed horizontally in its middle. On the side several waterproof doors are installed for better accessibility of the interior. The barrel is screwed watertight to the bottom plate. After unscrewing it can be removed by a crane permanently mounted to the wall of the observation room. The laser beam enters horizontally through a lateral flange and hits dielectric mirror which directs the beam vertically (see below). Inside, the case is equipped with thermostat-regulated heating to prevent condensate formation. The bottom plate on which telescope and multiplier unit are permanently mounted rests on three blocks attached to the floor of the observation platform and is provided with a leveling bubble for adjustment purposes.

4.2. Cassegrain Reflecting Telescope

A reflector of Cassegrain construction serves as receiving telescope. The main mirror has a diameter of 520 mm. Opposed to it is a convex collecting mirror installed in an adjustable mounting, to generate the secondary focus behind the main mirror. The equivalent focal lenght of the entire system is approx. 3.8 m. The optical system was made by D. Lichtenknecker, formerly Berlin, and is of astronomical quality, hence there is no need for stopping down of marginal zones. The circle of confusion diffusion within the secondary focus has a diameter

of only 1/100 mm. The exit window of the optical system is provided with an iris diaphragm for limitation of divergence, and a shutter which can be opened and closed electrically from the console at the operating bench. The dielectric mirror is installed above the collecting mirror which makes the laser beam emerge exactly on the telescope axis. Despite some disadvantages we chose this concentric arrangement to be able to receive signals from all ranges of interest without any readjusting.

4.3. Photomultiplier Unit

The signals are received by a photomultiplier (PM) Type RCA-7265 with ERMA III cathode which is located inside a commercial cooling box. In order to reduce inherent noise the PM can be cooled down to minus 20°C by Peltier elements. Cooling is switched on and controlled from the operating bench. The light enters the cooling box through a double-walled window which is evacuated to prevent condensate formation. In addition the front pane is heated. Also located inside the cooling box is an interference filter with its transmission maximum at the ruby wave lenght of 694.3 nanometers and a half-band width of 3.0 nanometers. Its purpose is to reduce background luminosity. To further reduce background noise this filter can be replaced, if required, by one with a half-band width of 1.0 nanometers which is, however, designed for a nominal temperature of minus 20°C. Outside the cooling box a polarizing is installed by which the degree of polarization of the backscattered laser light can be measured.For this purpose the cooling box is mounted in a rotary support.The angle of rotation can be read from a vernier scale.The Photomultiplier can be alugned with the telescope axis by two micrometer gauges standing at right angles. Finally, a wedge filter, which can be adjusted from the operating bench by a flexible shaft, is instal-

led in front of the PM entrance window. It is used to reduce background luminosity when operating with the t^2-control which is designed for a fixed PM high voltage of 1,500 Volts.

The PM is additionally equipped with the usual magnetic shielding. The previously mentioned deflection coil for the t^2-control, is inside the magnetic shilding. The dynodes of the PM are supplied with voltage in the usual manner by means of a voltage-divider resistor chain. The output signal voltage originating across a 10 kOhm resistor reaches the input of the oscilloscope via a sealed 75 Ohm cable.

5. First Experiences and Difficulties in Operating the System

The manufacturer of our Lidar system (Impulsphysik GmbH,Hamburg) has been engaged for a long time in the manufacture of units generating high-power electrical pulses for many applications, and recently for lasers used for a variety of purpose. Therefore, in designing our system they were able, to a large extent, to fall back on proven components which are being mass produced, particularly the entire electronic system and the laser head itself. This has proven very advantageous, especially from the point of view of reliability of the unit.

Nevertheless, the system in its entirety is an individual development. Therefore, certain initial problems could not be avoided. Although they have gradually been eliminated, the beginning of measurements was considerably delayed. It must always be borne in mind that in many respects we have gone the limit of what is technically permissible, particularly in regard to loading the optical components.

The technical alterations we were forced to make in the first months of operation have already been mentioned in the descrip-

tion of the system. Shortly after commissioning the system the ruby end faces were severely damaged twice in a row, each time necessitating time-consuming rework. The cause could not be completely clarified, but it is assumed that insufficient performance of the originally built-in air blower for the ruby end faces was to be blamed. (Although in the test run at the manufacturer's it had worked fine!). The end faces have remained perfect since dried and purified compressed air has been used.

A metal-like, mostly reddish deposition which,was easily removed, was repeatedly found on the flash lamp and the silver-coated mirror in the cavity of the laser head, drastically reducing luminous efficiency. It was first suspected that it was sputtered-off metal from the ignition wire of the flash lamp. Therefore, the lamp was sent to the manufacturer for examination. It is not yet possible to clearly ascertain the cause of this effect. It can be reduced by more frequently renewal of the water in the secondary coolant circuit. It is possible that the deposition consists of decomposition products of components of the PVC tubing dissolved in the water, which might form through the intense radiation of the flash lamp.

Temporary troubles were also experienced with the triggered spark gap for controlling the Kerr cell, where spray discharges occurred. They were eliminated by renewing the sealing compound in which the individual components are embedded.

As stated above, the afore-mentioned problems caused a certain delay in practical measurements, but contributed quite considerably - it must be said - to a deeper technical insight into the system. The experiences thereby gained should come in very handy in future research work.

6. Methods of Evaluation, Examples

As yet, evaluation of Lidar measurements must be done by measuring oscilloscope photographs on polaroid or standard film. Thus far we have worked with polaroid film only, as the equipment for loading the standard-film type camera back section, as well as for developing the films is not yet complete. Besides, we did not want to give up the advantage of immediate development of the pictures during the training period.

The oscilloscope traces are measured, point by point, on the photograph. The X-(time-) coordinate values are converted into altitude values by the pre-set time-base speed (1 μ sec corresponds to an altitude of 150 m). The Y- or signal intensity values are multiplied by the square of height (calculated from station point) in order to eliminate the decrease of intensity according to the R^2-law. Moreover, the values thus obtained are only relative values inasmuch as absolute calibration of the instrument has not yet been completed. This is planned for 1974.

Naturally, measuring of oscilloscope traces is very complicated and time-consuming. To facilitate this work a program was developed for our programmable desk computer. With its help the above mentioned conversions are performed, and the returned reflex signal profile, thus corrected, is plotted using the attached plotter. For an example we have selected the evaluation of several measurements made on 2 August 1973. On that day there was also a Rawinsonde ascent Fig. 29 shows the original photographs. The camera can be moved horizontally or vertically in a slide mechanism provided with lock-points, which permits including up to 9 oscillograms in one picture. The photographs are so aligned that the X- or time axis representing the height axis points up. The backscattering intensity (Y-axis of oscilloscope) is shown by the horizontal deflection of the curves rising to-

wards the right. For details see Table.

Data of exposures for Fig. 29

	X = altitude coordinate	Y = intensity coordinate
I :	a...e: 5 µs/cm corresp.to 750 m/cm	5 mV/cm
	f...h: 2 µs/cm corresp.to 300 m/cm	5 mV/cm
	i: 2 µs/cm corresp.to 300 m/cm	20 mV/cm
II :	a...b: 2 µs/cm corresp.to 300 m/cm	5 mV/cm
	c...d: 2 µs/cm corresp.to 300 m/cm	10 mV/cm
	e...f: 2 µs/cm corresp.to 300 m/cm	20 mV/cm
	g...i: 2 µs/cm corresp.to 300 m/cm	100 mV/cm
III:	same data as for Fig. ... II.	
IV :	a...f: 5 µs/cm corresp.to 750 m/cm	5 mV/cm
	g...i: 5 µs/cm corresp.to 750 m/cm	20 mV/cm

The scale of the Figures is 1:2, i.e. 5 mm on the Figures correspond to 1 cm on the oscillograph screen.

The traces used for numerical evaluation on photographs I to IV are marked by arrows.

Fig. 30 shows the reflection profiles put out by the plotter for the photographs so marked. On that day multilayer stratiform clouding (Sc, Ac), partly perforated, prevailed in the hours of the forenoon. The cloud bases which can be located by the particularly intense Lidar-returns, are shown in Fig.30. From the first three profiles in particular, two levels in an altitude of about 2,500 and 2,900 m a.s.l. are recognized where temporary stratification of clouding occurred. An interesting observation in this connection, which has been frequently made

on other occasions, is that increased backscattering may occur at this level even if no clouds exist in the beam direction. Undoubtedly this is a phenomenon of precondensation (growing of cloud nuclei when humidity is approaching the point of saturation), or a concentration of residual nuclei resulting from vaporization of cloud droplets.

Despite the initial difficulties mentioned in the preceding chapter, our observation material has already grown to much more than 300 polaroid photos, each of which reflects at least four individual measurements. A strictly qualitative examination of the material has already yielded an abundance of interesting observations, particularly in comparison with cable-car recordings. For example, we have found that haze layers (Lidar return maxima) are not always correlated with inversions. To investigate such phenomena more closely, a great number of individual measurements would have to be evaluated. Such evaluation, if carried out by the methods thus far practiced, would be impractical. In the long run, therefore, the acquisition of an electronic data handling system cannot be avoided. The wide dynamic range of the returned signal, a consequence of the R^2-law adds to the problem. An oscilloscope gain setting that is suitable for the weak signal from higher altitudes causes the stronger signal from short ranges to be off scale; if the gain is set correctly for the strong low altidude signal, the weak signal from higher altitude is insufficiently amplified and cannot be measured accurately. This problem is avoided by using the t^2-control within a certain distance range. However, this control can only be employed at nighttime. Otherwise, the constant background would also be multiplied by t^2 and obscure the actual signal. For this reason the acquisition of a suitable electronic system, consisting of fast operational amplifiers and function generators, effecting multiplication by t^2 between multiplier output and sequential electronic system, (data handling) is considered necessary.

7. Observationsat the 5th Laser-Radar Conference in June 1973

W. Carnuth participated in the "5th International Conference on Laser Studies in the Atmosphere", taking place in Williamsburg, Va., USA, from 6 to 8 June 1973. This was an excellent opportunity to obtain information on the state of the art and on development trends in this field.

The great importance lidar use hade recently achieved was reflected in the number of papers read which had increased to more than 70 from the 40 of the previous conference. As a consequence of the young age of lidar technology, the majority of the subjects covered new technical developments, partly just in the project stage; results of measurements were less frequent; least of all were results of continuous, systematic observations. The topics were subdivided into the following partly overlapping principal fields:

Laser-radar systems;
theory of elastic scattering;
stratospheric scattering measurements;
Raman, resonant and fluorescent scattering both in lab and field;
tropospheric scattering measurements and aerosol scattering.

Great effort is presently being made in the area of the Raman Lidar, a method which permits long-range measurements of trace gases and contaminant emission (chiefly SO_2 and nitric oxides), which are of importance in connection with efforts to reduce air pollution. The experimental difficulties to be overcome are enormous, mainly because of the weakness of measurable effects and because of the hard-to-eliminate background, e.g. due to aerosol fluorescence. High demands are made on the sensitivity of the equipment, which is why, thus far, measurements are

preponderantly made in areas with above-average concentration of the gases being studied, such as directly inside plumes of smoke or inside the exhaust gases of jet engines.

Actually there were just four papers discussing lidar measurements on stratospheric aerosols, which were of particular interest to us, namely by Hake and Co-workers (Standford Research Institute), Schuster and staff (NCAR, Boulder, 2 papers), and Rosen and Melfi (University of Wyoming/NASA Langley Res. Center). Although the group of the University of Kingston, Jamaica (Kent et al) working with the largest presently existing lidar (21 individual mirrors with a total receiver surface of 20 m^2, corresponding to an individual mirror of a 5 m diameter) also conducts continuous measurements in the stratosphere up to a height of 100 km, they were unable to distinguish any aerosols in the altitude range studied. However, Cohen (Jerusalem), whose paper was unfortunately cancelled, reported in his abstract successful stratospheric aerosol measurements. Schuster conducted measurements, both by Lidar on the ground, and with a relatively small Dye laser, from an airplane. Hake uses a 2 joule ruby laser with a Cassegrain 40 cm telescope as a receiver. Melfi had NASA's new big lidar available to him which has a cast metal mirror with a diameter of 120 cm, although the latter is not of astronomical quality. The Lidar measurements were, in part (Schuster, Melfi), compared with the global balloon measurements regularly conducted by the University of Wyoming using impactors and photoelectric counters. Rosen reported on this in an introductory paper. Agreement was found to exist to the extent possible.

Inasmuch as backscattering of stratospheric aerosols amounts to no more than 20% of the Rayleigh scattering by air molecules, the latter must be subtracted from the measured values to obtain just the aerosol share. This is done by calculating a

theoretically pure Rayleigh scattering curve, based on the atmospheric density distribution, and assuming that nothing but Raleigh scattering prevails in the region of minimum scattering below the stratospheric aerosol layer (Junge layer). Thus the ratio between theoretical and measured scattering intensity is put equal to one, for this altitude.

The measured values were exclusively obtained with the aid of electronic data logging systems. Generally, increased application of such systems was found to exist in all other fields of lidar application, as revealed by the papers. Basically there are two different methods: By the first, the analog signal supplied by the receiver (PM), is digitized and stored in a fast transient recorder with as many sequentially gated channels as possible. The signal, which is now broken down into a series of measuring points, is recovered from this transient recorder at a reduced speed, for computer processing.

The second method avoids the analog signal entirely, making use of the fact that actually the output signal of the PM is made up of individual pulses which are generated by a relatively small number of photoelectrons ejected by the cathode. These pulses can be counted by an adequate high-resolution electronic system (photo counter), and then immediately transient-recorded as with the former method.

The former method is less costly and simpler as commercially manufactured units can be employed. Units developed by the US company of Biomation for the measurement of short fluorescence decay times are used almost exclusively.

The photon count method is more sensitive and is employed to advantage for measuring low signal intensities where the signal is more and more resolved into individual pulses and a real analog signal is no longer coming about. E.g. Hake and colla-

borators who are employing both methods simultaneously, are reporting that the analog method can be used only up to 30 km height, and beyond that photon counting must be resorted to.

These considerations have a bearing on our work, also. Our first nighttime measurements up to high altitude have already shown the expected high resolution of the returned signal into individual pulses which, in practice, are manifested by a considerable broadening of the oscilloscope trace. In the interest of the greatest possible accuracy of measurement which is a necessity in view of the slight measuring effects to be expected, we will not be able, in the long run, to avoid applying the photon count method.

With the aid of electronic data recording systems it will be possible to handle even the wide dynamic range of the reflex signal. The signal attenuation which is due to the R^2-law can easily be compensated by computation. Collis (Standford Research Institute), for example, is using a function generator to generate the function of 2 ln R (= ln R^2) which is then added to the logarithm of the measured signal. This is why direct amplification controls of the PM (so-called t^2-controls) were no longer discussed by any of the papers. The computation method of eliminating the R^2-law does not, however, avoid another problem which may be caused by the intense short-range-signal, viz. the overdriving of the PM. The Kent group has made a close study of this effect which makes itself conspicuous by a transient decrease in sensitivity and increase of dark current. As a desirable side effect our t^2-control largely avoids such phenomena of overdriving.

Most lidar systems are equipped with a transmitter telescope (usually a simple Galilean telescope) to reduce beam divergence. Initial talks have been conducted with the manufacturer concerning the acquisition of such a telescope for our

unit, too. It is true, however, that with our system beam divergence is already rather small (1.5 mrad), due to the relatively large lenght of the laser resonator permitted by the fixed arrangement we have.

Scatter measurements on tropospheric aerosols which are also very important to us, are much more frequent than stratospheric scatter measurements. McCormick (NASA Langley R.C.) reports on simultaneous measurements by impactors from airplanes (conducted by Blifford, NCAR Boulder). They used a ruby laser with frequency doubler. Usually KH_2PO_4 crystal will serve this purpose. The double-frequency method permits one to obtain information on the size distribution of the aerosol, something which is impossible with just one frequency. For the same reason, the tunable dye laser is also used for such purposes.

Information on aerosol size distribution may also be obtained by measuring the angular distribution of the scattered light by a so-called bistatic lidar with which one does not measure in the 180° direction only, as is done with the monostatic lidar. Certain theoretical problems are, however, caused by deriving the size distribution function from the scatter function. Several papers delt with this subject, frequently having to make simplifying assumptions.

Ultimately, polarization measurements, too, can yield certain information as to aerosol size distribution (Cohen, Jerusalem), More exactly speaking, what is measured is the depolarization of the scattered light generated by a polarized laser beam. This depolarization is controlled by certain properties of the aerosol particles. The depolarizing effect of various types of clouds, however, is much stronger due to multiple scattering. (Alishouse, NOAA Maryland; Harris/McCormick). Multiple scattering in forward direction will also cause an increase in the transmissivity of clouds (Werner, DFVLR).

Observations of turbulence in the atmospheric ground stratum by means of visualizing aerosol inhomogeneities through the scanning method, that were conducted at the Stanford Research Center, were quite impressive. This method converts reflected intensities into screen intensities as has long been customary in radar technique. Thus an immediately illustrative impression may be obtained of aerosol stratification relative to time and space (lidar mounted on vehicle!). A comparison using an acoustic radar which, in contrast to the optical one, responds to inhomogeneities of temperature is also very informative. Thus it was possible to observe very nicely how, for example, the lidar will show newly formed inversions only after sufficient aerosol has accumulated beneath the barring layer.

Also used for observing atmospheric turbulences is the Doppler Lidar (Schwiesew, NOAA Boulder, and Fiocco, Florence, Italy). Movements of the backscattering aerosol particles make themselves conspicuous by line shifts in the scattered light as compared to the laser line. It is possible, to separate the signal shift into a mean value (wind velocity!) and a fluctuation about the mean. This fluctuation is caused by turbulence. From this and the vertical gradient of aerosol concentration it is possible to calculate the exchange coefficient.

Several interesting papers concerning these subjects had been announced from the Soviet Union which, however, were unfortunately cancelled, except one.

In the way of further applications let us mention measurements of visual range (McCormick) and of rain intensity (Eloranta, University of Wisconsin).

The 6th Lidar Conference is planned to take place in Sendai, Japan, from 2 to 5 September 1974.

8. Summary of the critical examination of our Lidar system and necessary further extensions.

Compared with other lidar equipment at work or in progress, we can state that our system in its basic concept is well suited for aerosol scattering studies in the near ground layer as well as in higher altitudes up to 15 km or so. It has good receiver sensitivity, because of the telescope size, good power output, and a high maximum pulse repetition frequency.

Nevertheless, for maximum performance several extensions seem to be necessary to complete the setup:

a) Absolute calibration or at least normalisation of both the laser transmitter and receiver.

To measure the laser output energy, a specially designed calorimeter has been ordered and is now available. This device gives the energy per pulse in absolute units (joules), but due to its long cooling time and the fact that all the energy of the laser pulse is consumed for the measurement, it is not suitable for routine normalisation measurements. Therefore, an additional light meter containing a fast photodiode has been ordered for the measurement of the intensity of each individual output pulse. This is necessary because of the considerable scatter of the pulse amplitudes. The photodiode device gives only relative values, but may easily by calibrated by means of the calorimeter.

The calibration of the receiver is a much more difficult problem. As a first step, a flashlamp designed for high speed photography has been purchased. This lamp has .8 microseconds minimum flash duration and a built-in delay time generator, continuously adjustable from 10 microseconds to 10 milliseconds.

This flashlamp is especially suitable for checking the performance of the t^2-control unit and to readjust it if necessary. Besides this, it should be possible to check the photomultiplier for long-time sensitivity variations.

b) Frequency doubler.

To get information about the particle size distribution of an aerosol to be measured, the return signal from at least two wavelengths is to be received. For this purpose, a KDP frequency doubler has been orderd. Its installation will involve a considerable amount of change in the mechanical construction of the receiver. Since the KDP crystal deflects the laser beam a little bit, a second deflection mirror is needed to maintain the capability of changing quickly from one wavelenght to the other. Also the interference filter in front of the photomultiplier, which is now mounted inside the cooling box, has to be interchangeable quickly.

Since the return signal in the double ruby frequency, i.e. near ultraviolet region, is mainly rayleigh scattering, it is well suited for normalisation of the whole system.

c) electronic data acquisition system.

As a first step, a biomation 8100 transient recorder with 8 bit resolution, 2000 word memory has been ordered together with a Facit tape punch and proper interface. This equipment,which will be available at the beginning of December 73, will lead to a considerably improved measuring accuracy and save a lot of

data reduction time.

The second step should be a photon counting system with range gating facility to increase the accuracy in assessment of weak return signals from higher altitudes.

VII. EXAMPLE FOR AN INITIAL COMPARISON BETWEEN LIDAR-REFLEX INTENSITY PROFILE AGAINST PROFILES OF CONDENSATION NUCLEI AND AEROLOGICAL DATA, OBTAINED BY ZUGSPITZE CABLE CAR TELEMETRY SYSTEM.

As pointed out in chapter VI. the LIDAR system has only just become operable. There are still some improvements and refinements to be made which only now can be accomplished step by step. Nevertheless, we have now started conducting systematical comparisons between LIDAR reflex intensity profiles on the one hand, and the simultaneously performed aerosol measurements at our three stations (Zugspitze peak, Wank peak and valley floor), plus the profiles of nucleus concentrations and aerological data obtained by Zugspitze cable car system, on the other hand.

This report presents a first example. Fig. 31 is a plot of the following as functions of height [+]):

a) LIDAR reflex intensity profile (relative units);

b) Concentration of nuclei calculated on the recorded air conductivity data by the methods customary up to now and in general use (cf. Reports V and VI). The logarithm of particles/cm^3 has been plotted;

[+]) Representation of LIDAR reflex intensity is here limited to a height up to 3 km.

c) Relative humidity (dotted line: values recorded 100 min. later by our RAWINSONDE in free flight);
d) Temperature and water vapor pressure (dotted line: temperature values obtained by RAWINSONDE 100 min. later).

It is obvious that the LIDAR reflex peak at 2,400 m a.s.l. coincides with a maximum of condensation nucleus concentration and relative humidity at exactly the same altitude (the temperature shows a less distinct minimum). It is evident, however, that nucleus concentration systematically increases already from 1,900 m a.s.l. on (relative humidity from 2,000 m on), without the LIDAR reflex intensity noticeably reacting. Obviously we are encountering predominantly very small and optically ineffective particles in the range between 1,900 and 2,300 m a.s.l.

Between 2,500 m and 2,650 m a.s.l. the LIDAR reflex signal is getting weak again: in this layer a minimum of nucleus concentration and (less distinct) of relative humidity is found, and also a slight temperature maximum. Above 2,650 m, LIDAR reflex intensity shows a sharp increase because a local cloud was forming at the altitude, which did not exist in the range of the Zugspitze cable car line (rel. hum. 60%). Yet at 2,650 m a.s.l. a distinct maximum of nucleus concentration is found, hence within the same range where cloud formation occurred. Interesting enough, a distinct maximum of LIDAR reflex intensity (LIDAR-shot of 0845, dash-and-dot line) had preceded said cloud formation at 2,650 m a.s.l.

No further inferences are drawn from Fig. 31. We are now commencing a program of systematically gathering LIDAR data and equally systematically comparing them against the aerosol data measured at the stations; as well as against those obtained by cable car telemetry system, and finally against the aerological data obtained by the latter and by the RAWINSONDE.

we realize that this very extensive work can only be done on the basis of electronic data processing for the LIDAR measured values, too, which is to be procured (basic funds) and taken into operation as quickly as possible.

VIII. CONCLUSIONS

The new Institute building taken into possession during the reporting period, offers an abundance of new and most modern research facilities in the field of atmospheric physics. Two large-scale systems for deepened investigation into the vertical aerosol distribution and its meteorological control up to an altitude of at least 30 km have been procured, installed and taken into operation, viz.

1) RAWINSONDE; this system for recording temperature, humidity, wind direction and velocity up to 30 km a.s.l. is fully operable.

2) LIDAR; the LIDAR system for plotting aerosol profiles up to at least 50 km a.s.l. is basically complete and ready for operation. Following improvements and additions will be effected (from basic funds) in the course of the next months;

   a) Installation of a Galilean telescope to improve beam divergence;

   b) Construction of a device for absolute measurement of LIDAR reflexes, consisting of
      calorimeter (to measure the effective laser energy),
      luxmeter (calibration of multiplier);

   c) Automatic data processing of received LIDAR signals and out-put in a defined manner on tape, for further processing by means of institute-owned computer system.

Initial data show interesting correlations between LIDAR reflexes and actually measured aerosol profiles.

The new facilities seem to be suitable to attain the objective set for our research, viz.

1) absolute calibration of the LIDAR system;

2) its application for continuous recording of aerosol distribution and its variations up to higher altitudes; also to study the controlling atmospheric-physical conditions and processes in troposphere and lower stratosphere. Problems of cloud formation and dissipation are also included.

IX. FUTURE PLANS

1. Work Exclusively Based on the Data from our Telemetry System

During the next months the work listed under 1.a to 1.e in Report VI, page 50, will be made up for, step by step, or continued. The introductory chapter of the present report shows and explains why this work had to be postponed for some time.

2. Direct Measurements of Profiles of Condensation Nucleus Concentration

It has already been mentioned under 1.f in Report VI, page 52, that we intend to instal a condensation nucleus counter in the Zugspitze cable car for direct recording with our telemetry system of the vertical profiles of condensation nuclei. Early

in 1973 we have ordered, from basic funds, the necessary microminiature model of a condensation nucleus counter, from General Electric, USA. The instrument should be delivered in fall of 1973. It will then promtly be installed in our telemetry system.

3. LIDAR System

a) The technical improvement and development of our LIDAR system, particularly its absolute calibration, as stated under VI., is to be carried out.

b) Notwithstanding that, aerosol profiles are to be contiuously recorded with this system, depending on weather conditions, to be manually evaluated for the time being, and to be compared with the aerosol profiles and aerological data supplied by our Zugspitze telemetry system. At the same time, aerosol measurements at our mountain stations are to be included also.

c) Procurement and commissioning of an electronic data processing unit for LIDAR signals, and development of suitable methods of computing for statistical evaluation and automatic analysis of correlation between LIDAR data and data by the telemetry system.

d) Expansion of studies on aerosol structure and aerosol transport up to at least 30 km a.s.l., based on findings per b) and c), above, utilizing the RAWINSONDE data.

e) Theoretical treatment of data, and parametrization.

f) Special studies into cloud formation and dissipation, employing all of our facilities and all findings gathered.

g) Special studies into the jet stream and the atmospheric-tropospheric exchange of air masses.

4. RAWINSONDE

Employment of RAWINSONDE within the scope of our LIDAR studies (cf. 2.c) through g) above) up to at least 30 km a.s.l..

Specific studies with the aid of the RAWINSONDE:
Execution of the project outlined in Report VI on page 54 XI. 4:

with the aid of our RAWINSONDE and the computer system we will attempt automatic electronic application of our parametrization functions with the aim of developing "pre-fabricated" computer programs for direct employment in practical use, both military and civilian.

X. REFERENCES

1) Reiter, R., R. Sládkovič and W. Carnuth

Atmospheric aerosols between 700 and 3000 m a.s.l., Part IV, A Study of effects of atmospheric fine structure characteristics in the vertical distribution of aerosols.
Final Technical Report, Contract DAJA-37-69 C-1357, July 1970.

2) Reiter, R., R. Sládkovič and W. Carnuth

On fine structure and control of vertical aerosol exchange between 700 and 3000 m; New method and results.
Arch. Met. Geophys. Bioklim. Ser. A, 20, 115 - 157 (1971).

3) Reiter, R. and R. Sládkovič

Control of vertical transport of aerosols between 700 and 3000 m by the lapse rate and fine structure of temperature: results of a sequence of measurements covering several years.
Journal of Geophys. Res. 75, 3065 (1970), CACR Symposium Heidelberg 1969.

4) Reiter, R., R. Sládkovič and W. Carnuth

Atmospheric aerosols between 700 and 3000 m a.s.l., Part V, A Study of effects of atmospheric fine structure characteristics in the vertical distribution of aerosols.
Final Technical Report, Contract DAJA-37-70C-2647, July 1971.

X. REFERENCES

1) Reiter, R., R. Sládkovič and W. Carnuth

Atmospheric aerosols between 700 and 3000 m a.s.l., Part IV, A Study of effects of atmospheric fine structure characteristics in the vertical distribution of aerosols.
Final Technical Report, Contract DAJA-37-69 C-1357, July 1970.

2) Reiter, R., R. Sládkovič and W. Carnuth

On fine structure and control of vertical aerosol exchange between 700 and 3000 m; New method and results.
Arch. Met. Geophys. Bioklim. Ser. A, 20, 115 - 157 (1971).

3) Reiter, R. and R. Sládkovič

Control of vertical transport of aerosols between 700 and 3000 m by the lapse rate and fine structure of temperature: results of a sequence of measurements covering several years.
Journal of Geophys. Res. 75, 3065 (1970), CACR Symposium Heidelberg 1969.

4) Reiter, R., R. Sládkovič and W. Carnuth

Atmospheric aerosols between 700 and 3000 m a.s.l., Part V, A Study of effects of atmospheric fine structure characteristics in the vertical distribution of aerosols.
Final Technical Report, Contract DAJA-37-70C-2647, July 1971.

5) Reiter, R., R. Sládkovič and W. Carnuth

Atmospheric aerosols between 700 and 3000 m a.s.l., Part VI, Parameterization of aerosol eddy diffusion controlled by aerological parameters.
Final Technical Report, Contract DAJA-37-71C-3210
February 1973

6) Reiter, R., R. Sládkovič and W. Carnuth

Parameterization of aerosol eddy diffusion controlled by the aerological structure.
Archiv für Meteorologie, Geophysik und Bioklimatologie
In press.

XI. APPENDIX

1. Figures 1 - 31

2. Tables I - XII

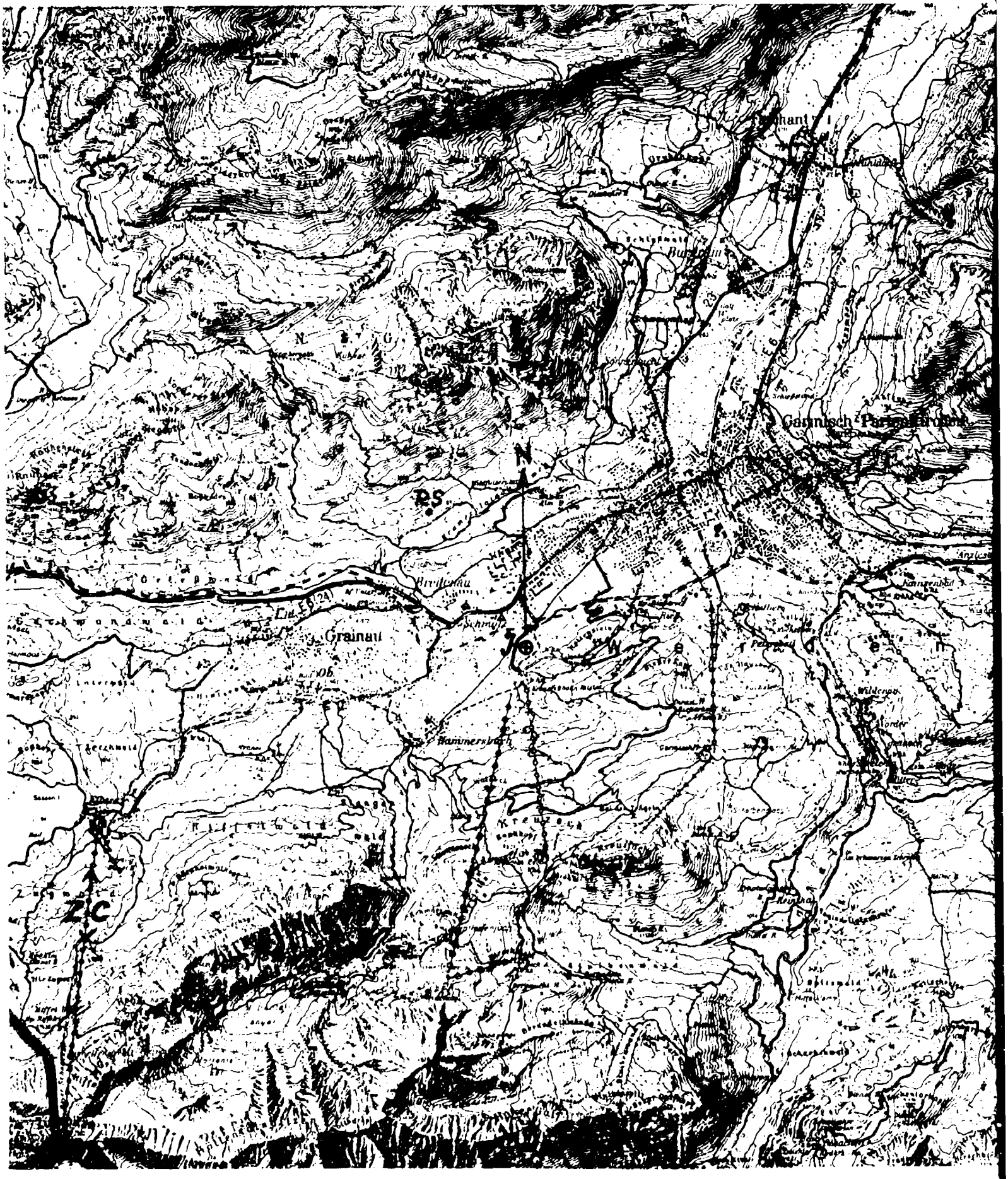
Grainau
Hammersbach
Garmisch-Partenkirchen


Fig 1
Garmisch-Partenkirchen
1:50000 (2 cm der Karte = 1 km in der Wirklichkeit)
0
2
4 km

Fig. 3

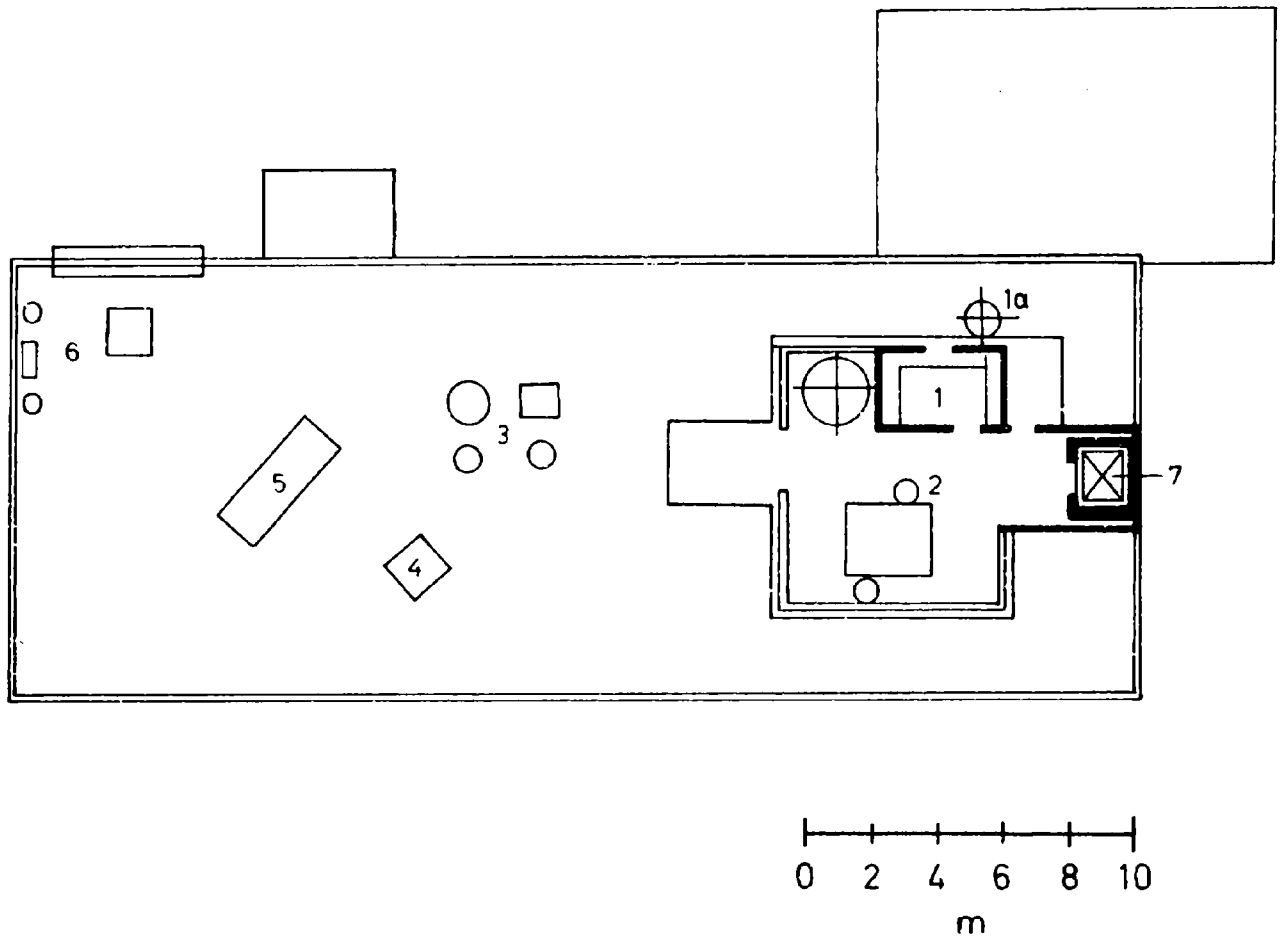

63

Fig. 5

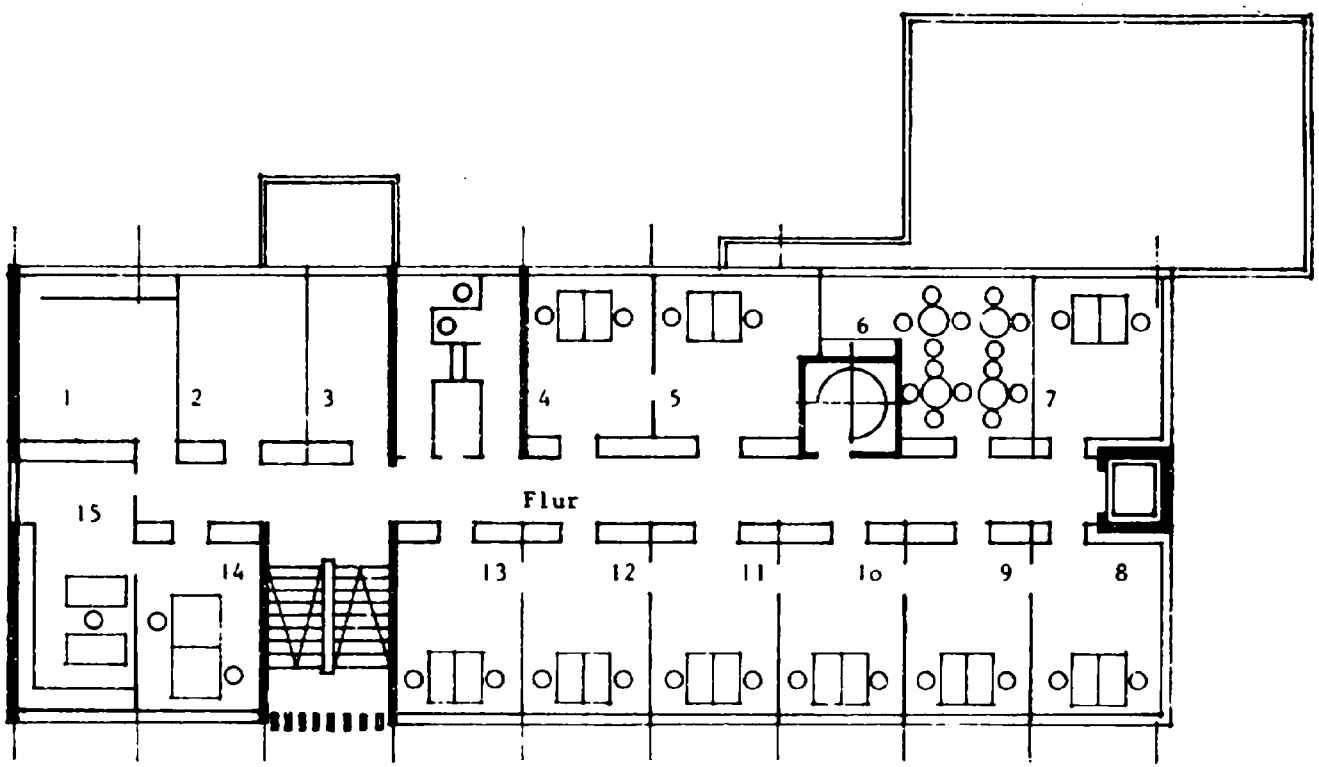

Fig. 9

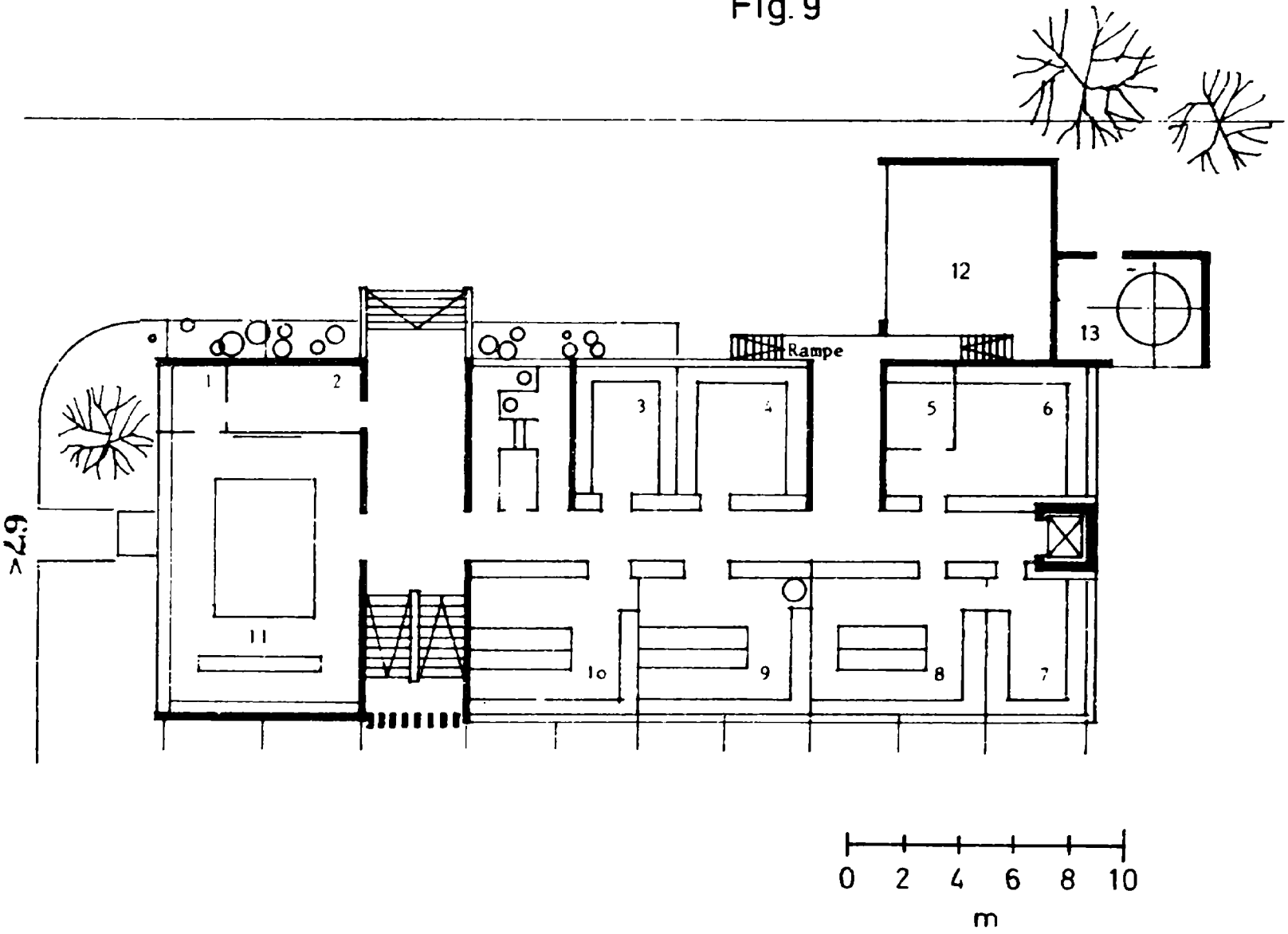

Fig. 11

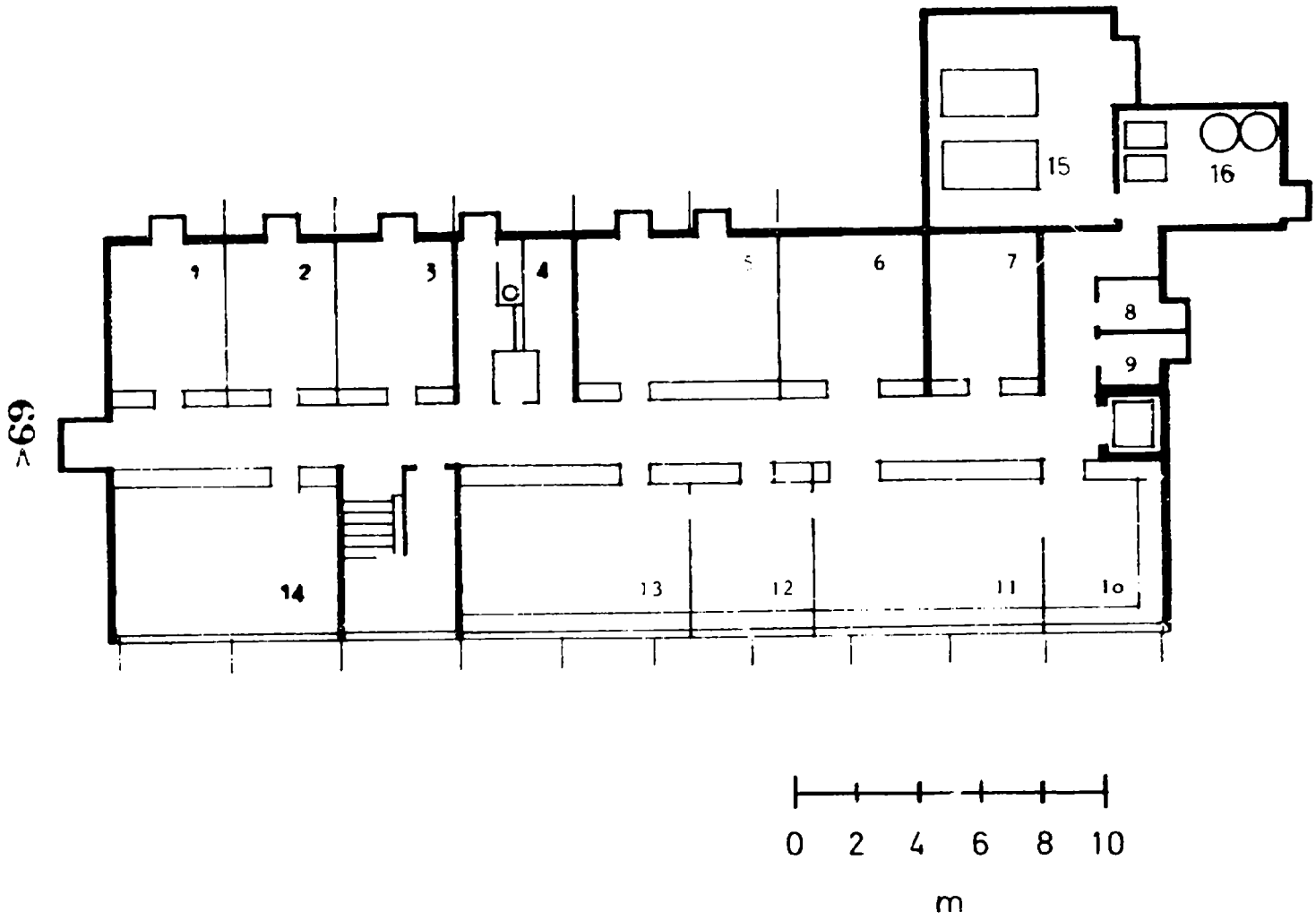

FIG.13

BALLOON ASCENT

10.08.1973 08.40 GMT

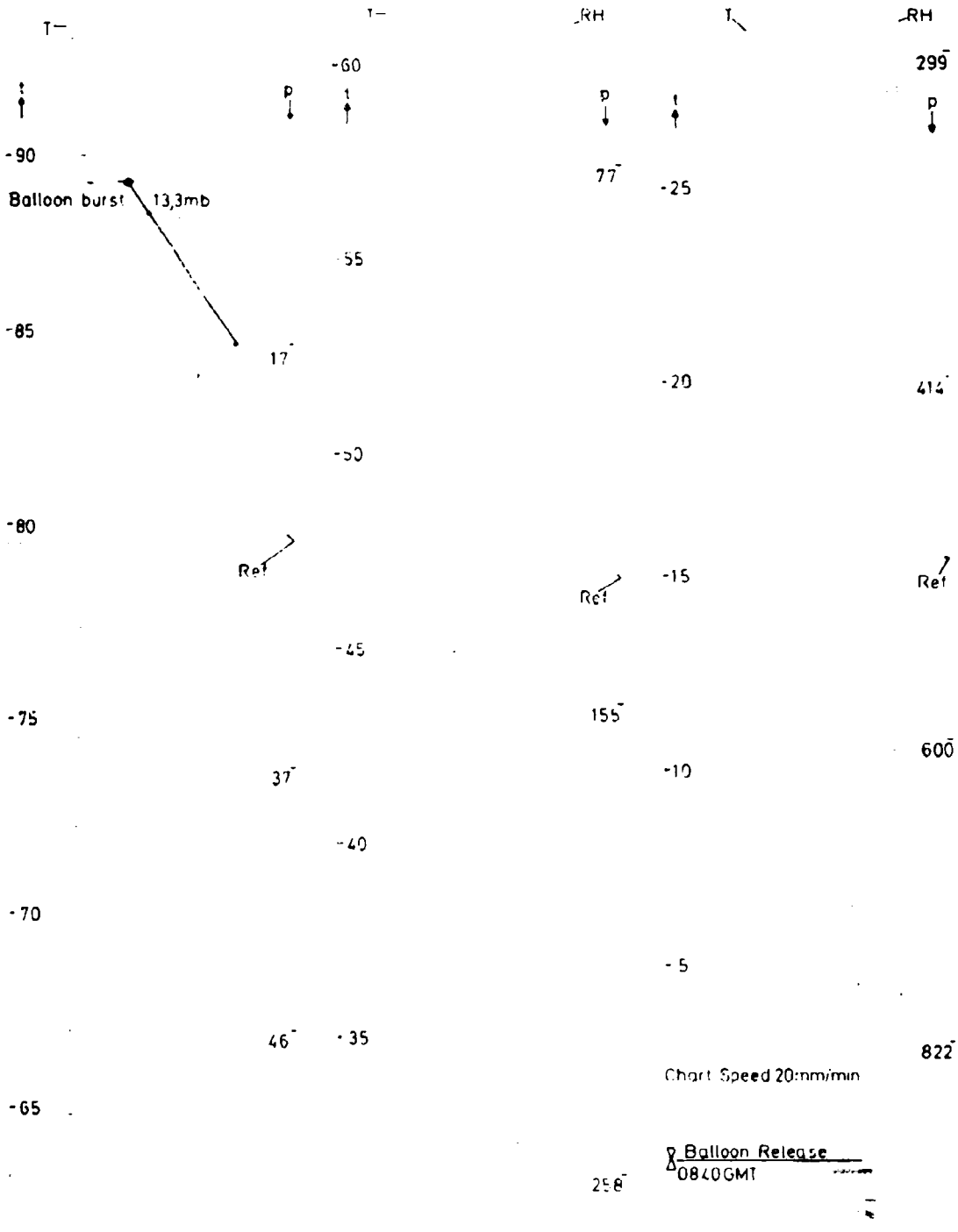

T Temperature °C p Pressure mb RH Rel Humidity %

Ref Reference t Time since Balloon Release min

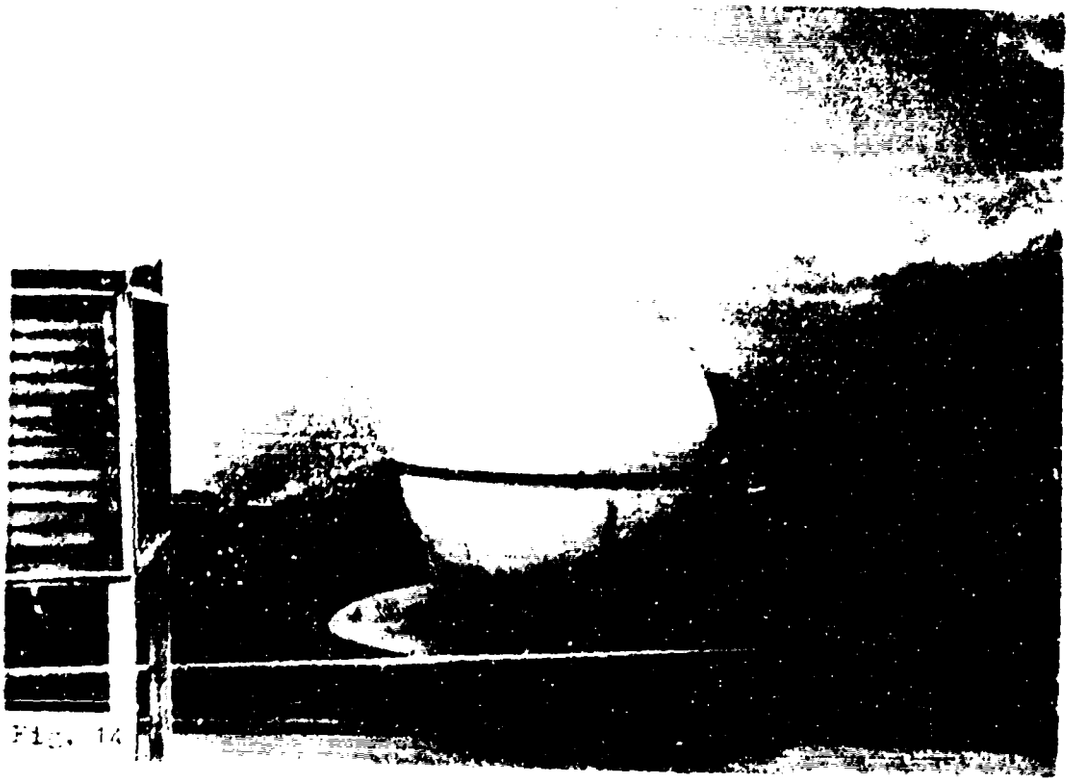

Fig. 14

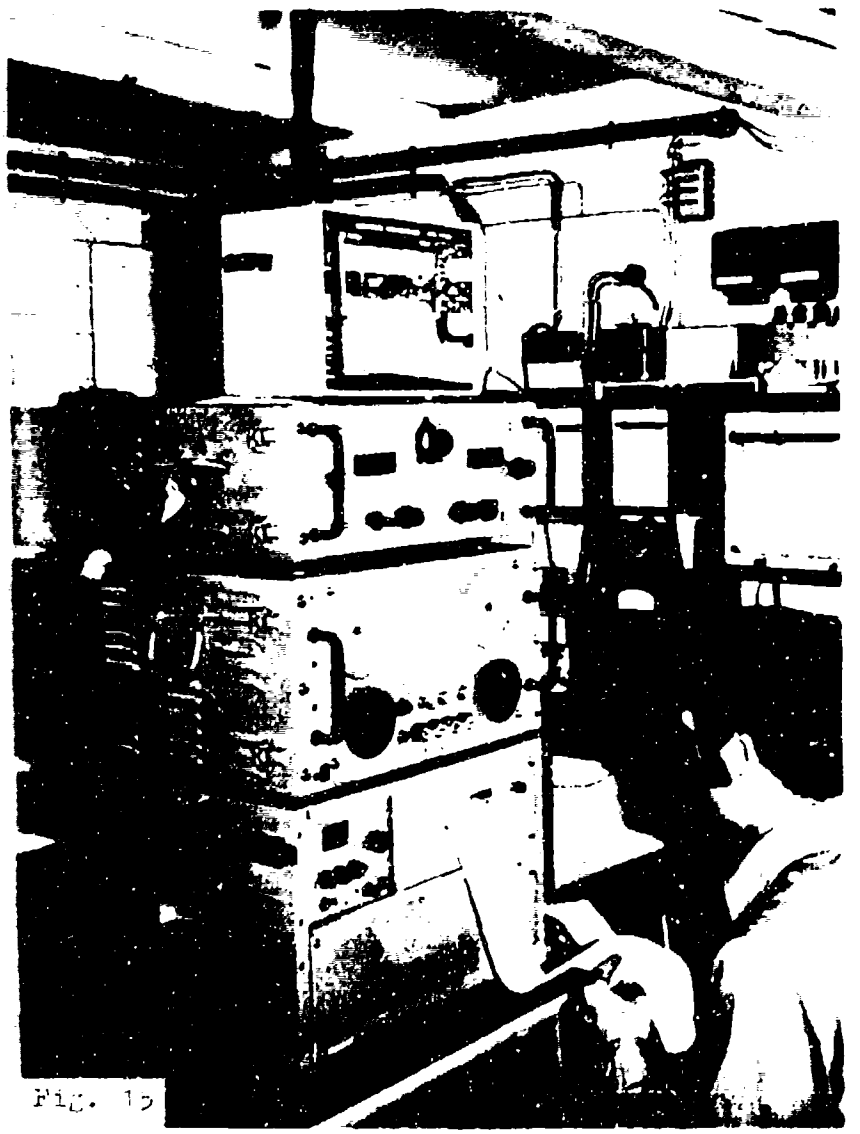

Fig. 15

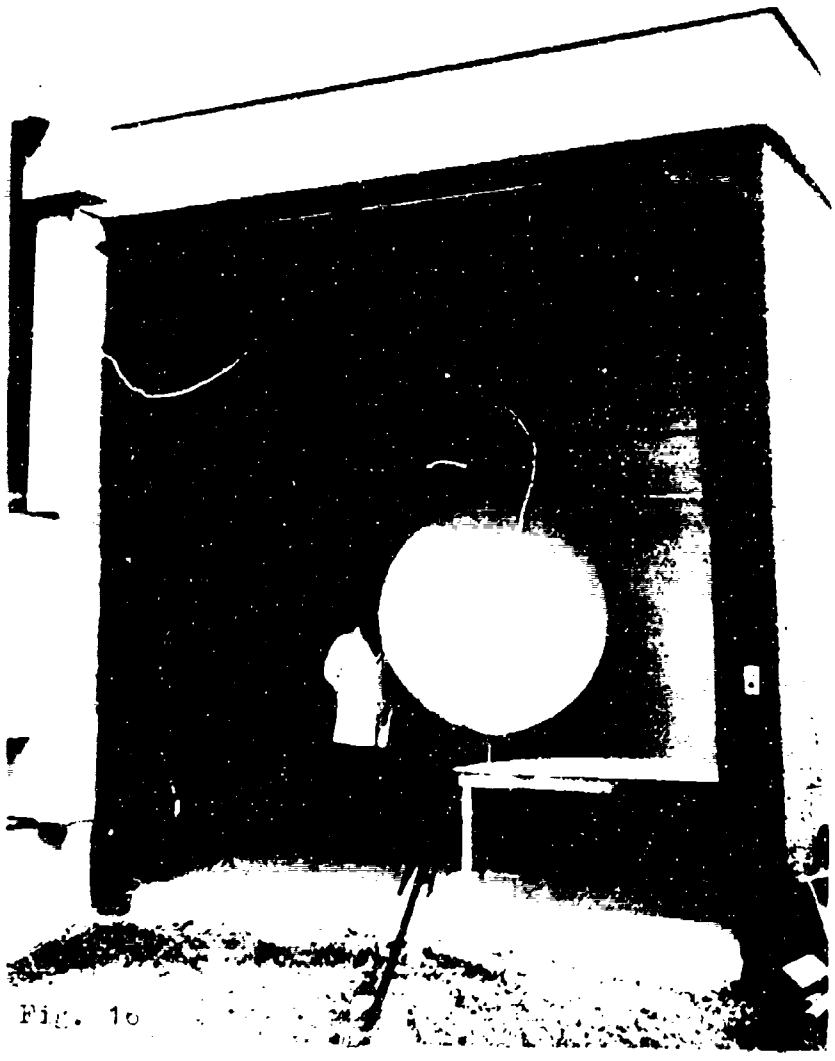

Fig. 1c

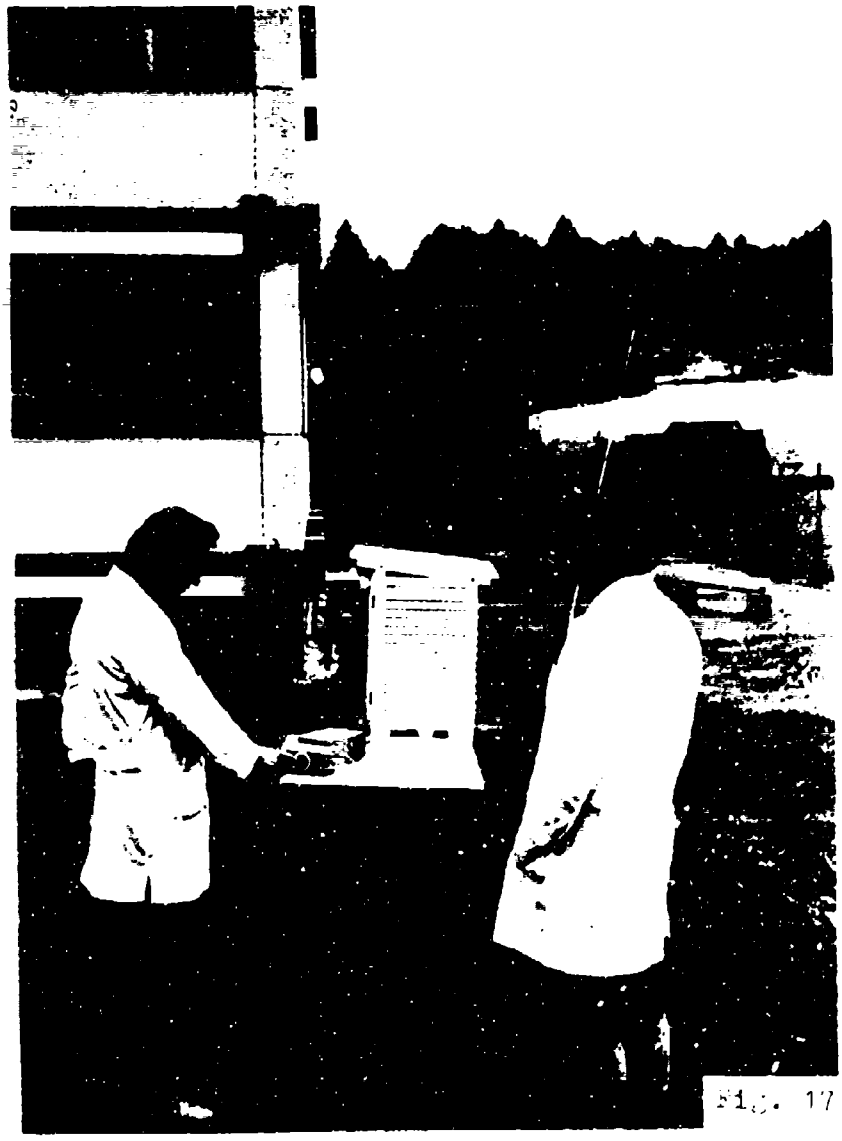

Fig. 17

Fig. 1

Fig. 1y

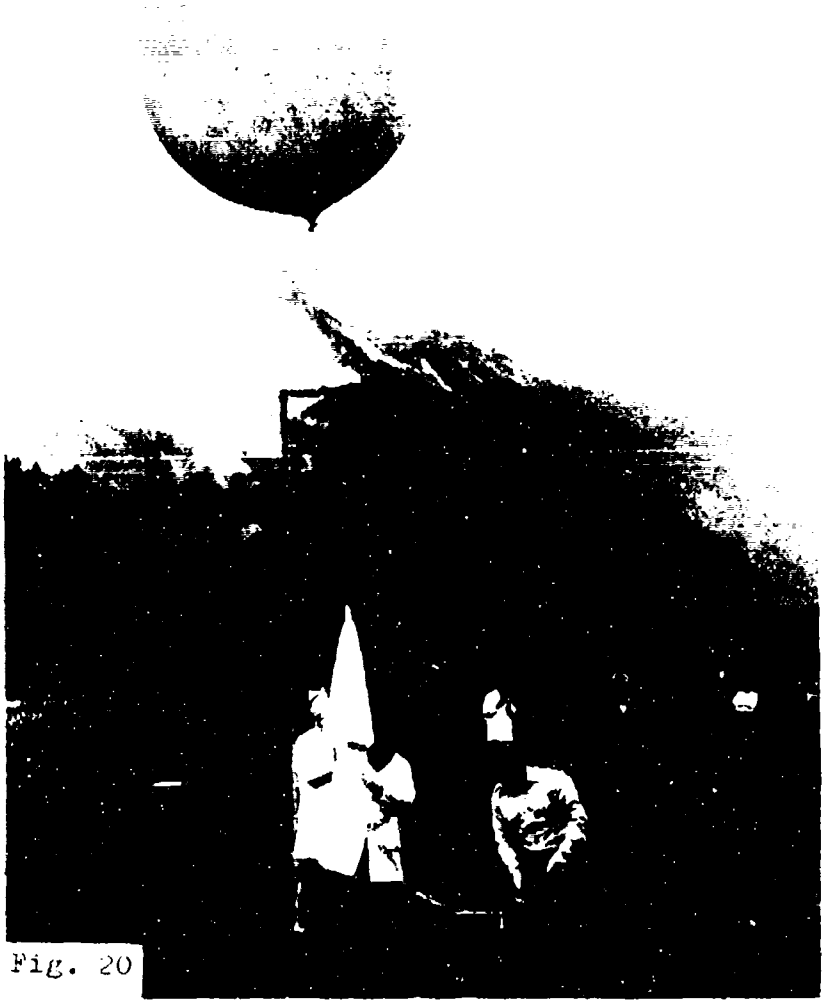

Fig. 20

Fig.21

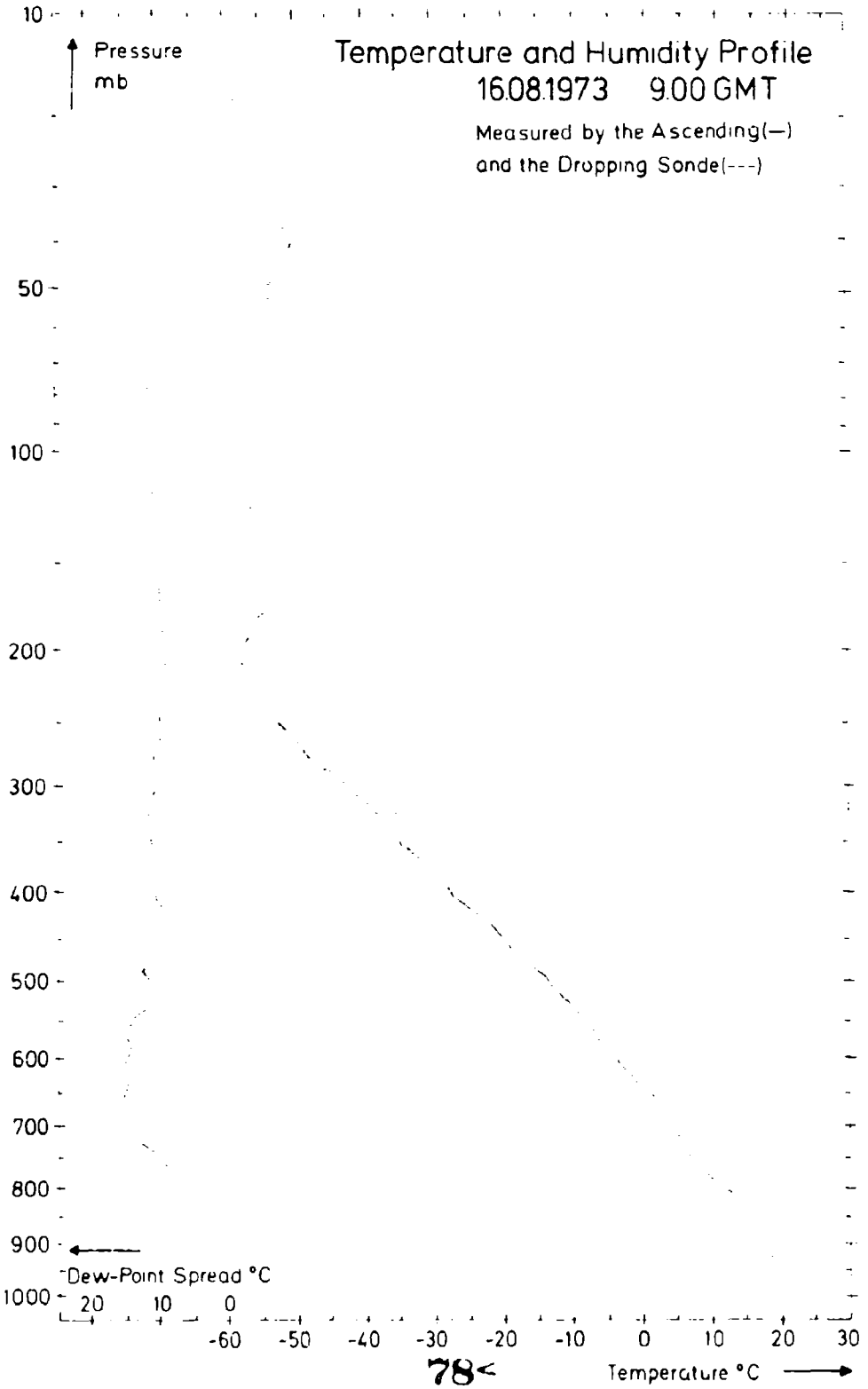
Temperature and Humidity Profile
16.08.1973 9.00 GMT
Measured by the Ascending(—)
and the Dropping Sonde(---)
Pressure
mb
10
50
100
200
300
400
500
600
700
800
900
1000
Dew-Point Spread °C
20
10
0
-60
-50
-40
-30
-20
-10
0
10
20
30
Temperature °C

Fig.22

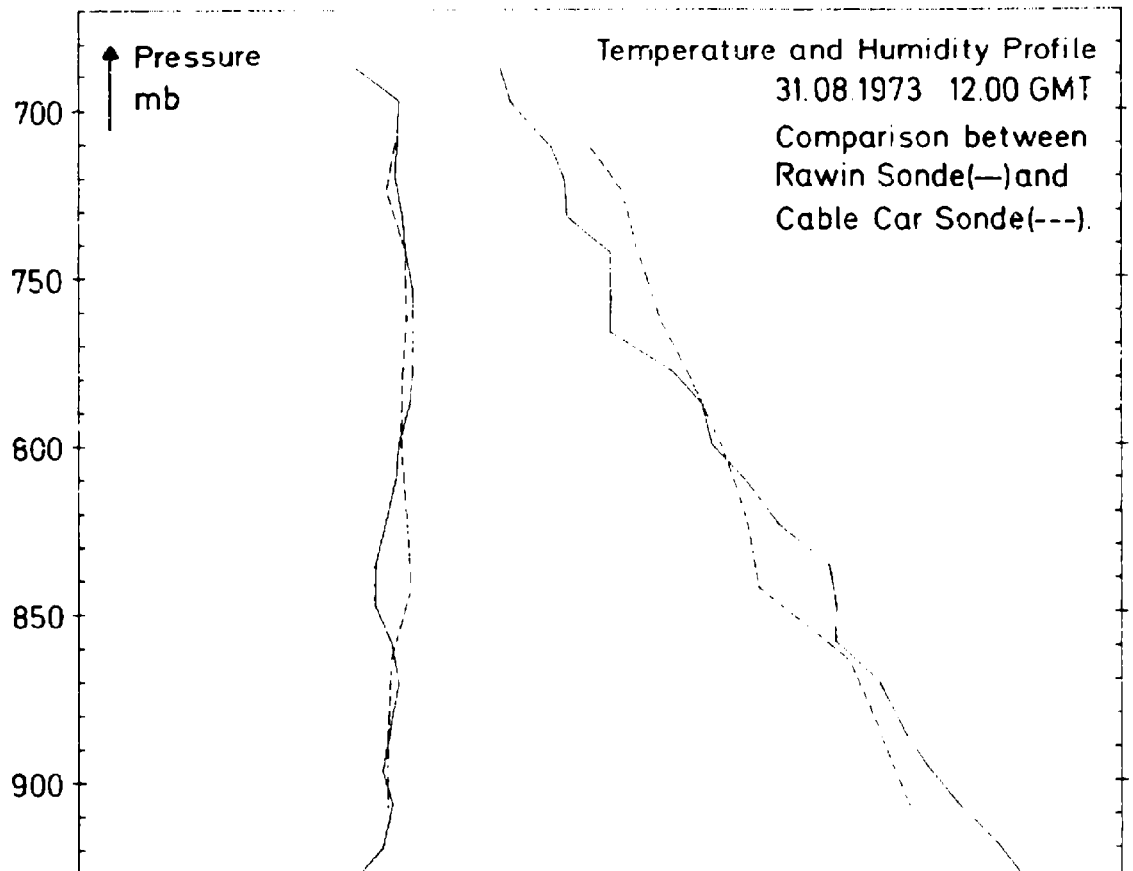
Pressure
mb
Temperature and Humidity Profile
31.08.1973 12.00 GMT
Comparison between
Rawin Sonde(—)and
Cable Car Sonde(---).
700
750
800
850
900
950
Rel.Humidity %
0 20 40 60 80 100
-5
0
5
10
15
Temperature °C

Fig.23

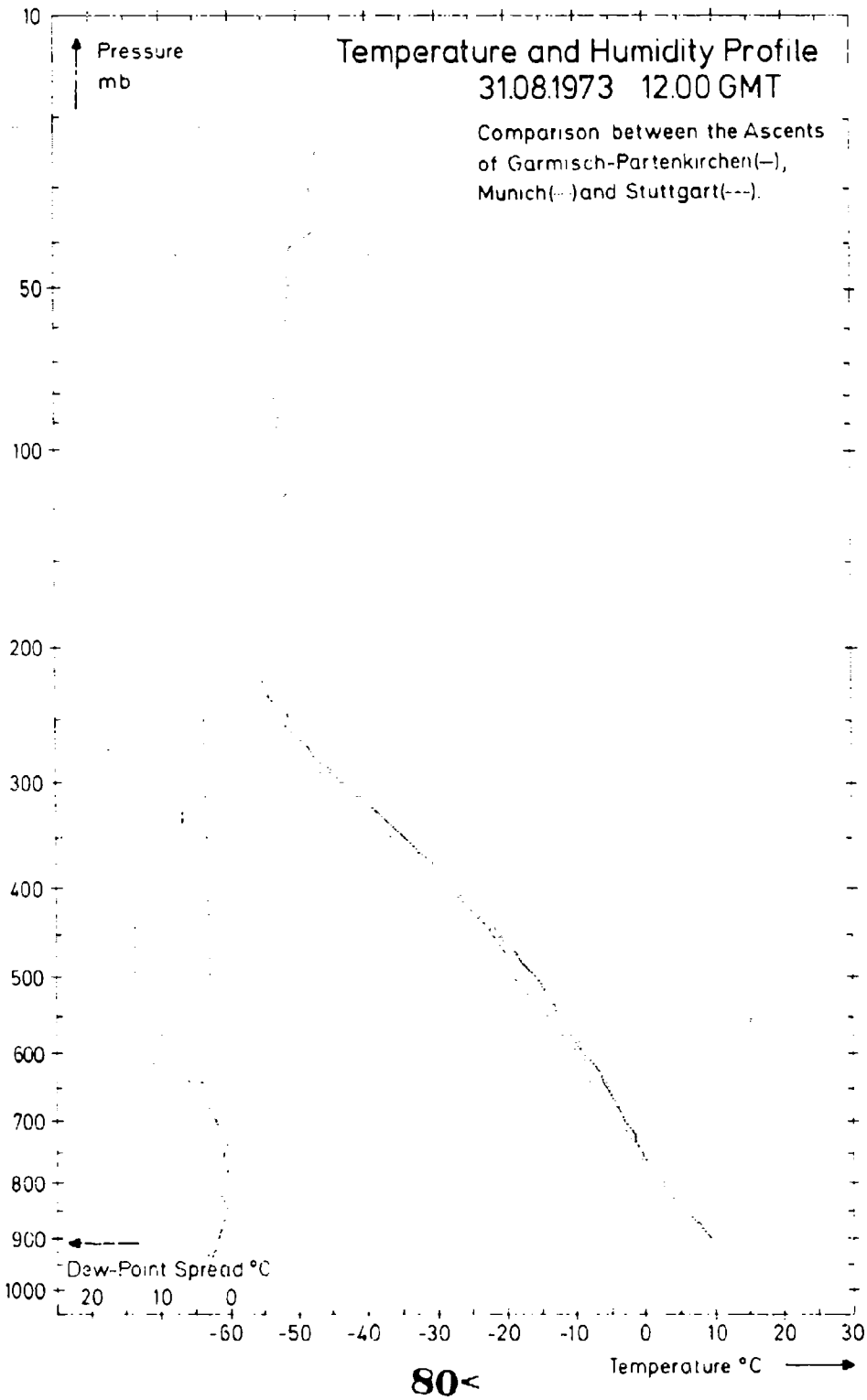
Temperature and Humidity Profile
31.08.1973 12.00 GMT
Comparison between the Ascents of Garmisch-Partenkirchen(—), Munich(··)and Stuttgart(---).
Pressure mb
10
50
100
200
300
400
500
600
700
800
900
1000
Dew-Point Spread °C
20 10 0
-60 -50 -40 -30 -20 -10 0 10 20 30
Temperature °C

Fig. 24

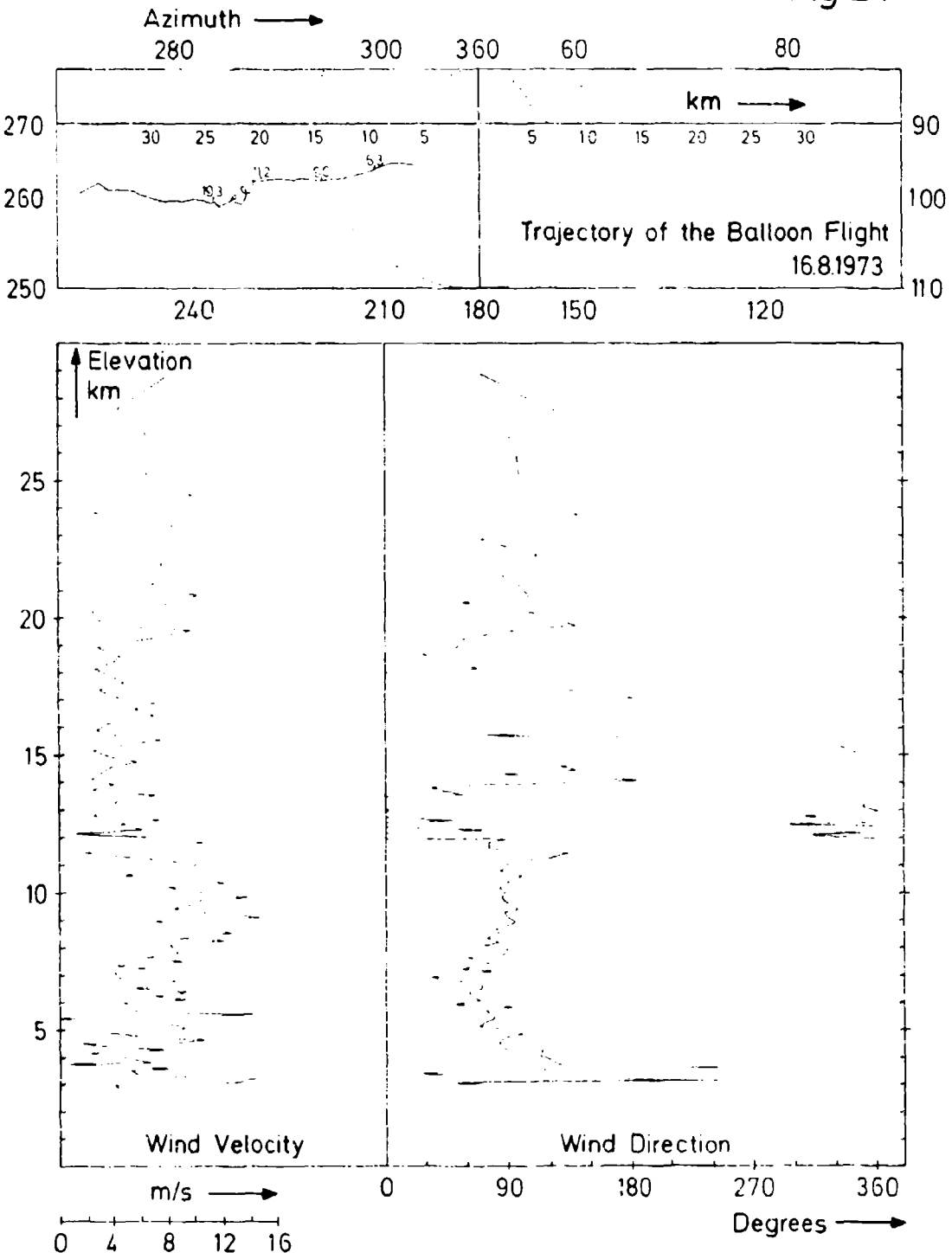
Azimuth
280
300
360
60
80
km
270
260
250
90
100
110
30 25 20 15 10 5
5 10 15 20 25 30
Trajectory of the Balloon Flight
16.8.1973
240
210
180
150
120
Elevation
km
25
20
15
10
5
Wind Velocity
Wind Direction
m/s
0 4 8 12 16
0 90 180 270 360
Degrees

Fig. 25

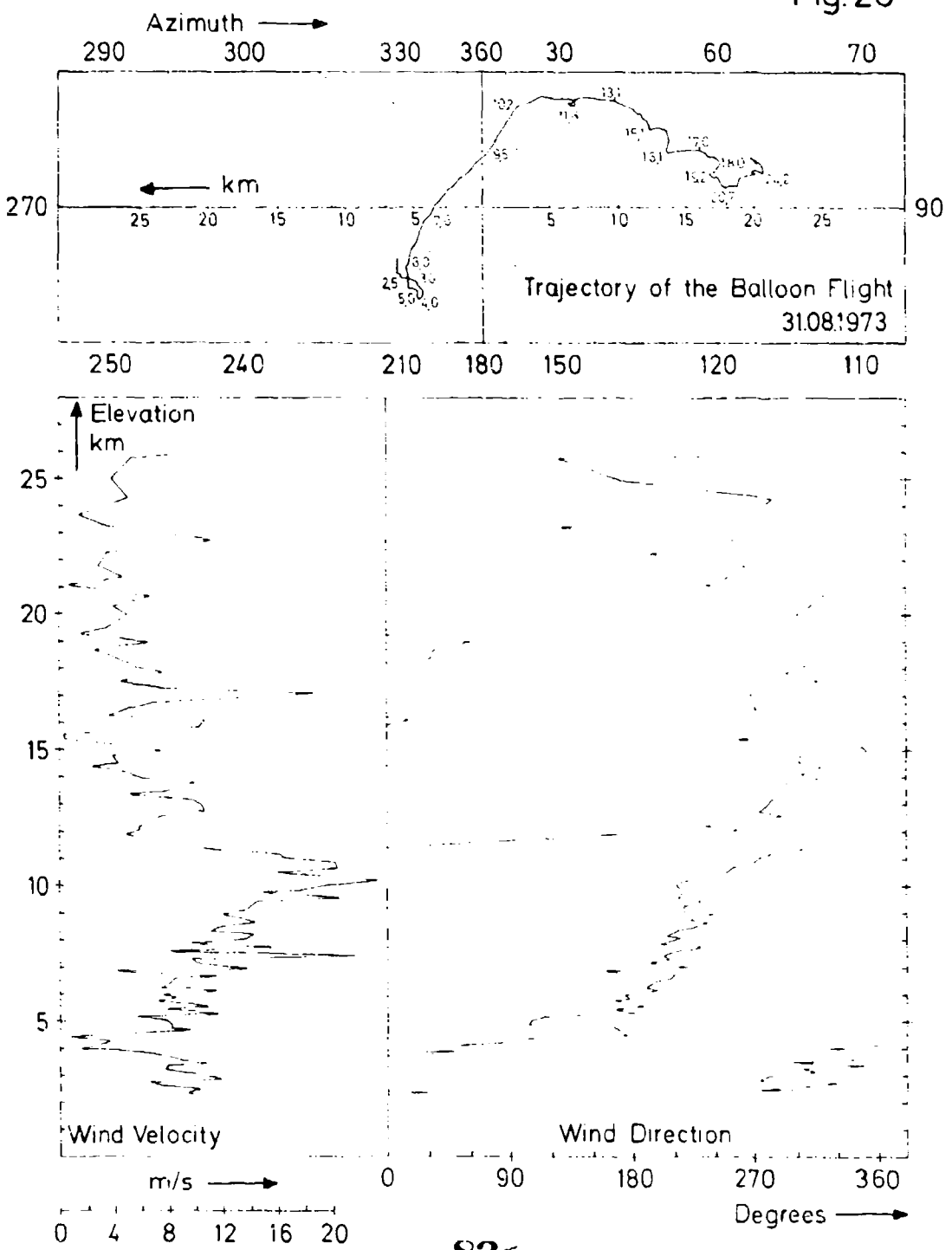
Azimuth
290
300
330
360
30
60
70
km
270
90
25
20
15
10
5
5
10
15
20
25
Trajectory of the Balloon Flight
31.08.1973
250
240
210
180
150
120
110
Elevation
km
25
20
15
10
5
Wind Velocity
Wind Direction
m/s
0
4
8
12
16
20
0
90
180
270
360
Degrees

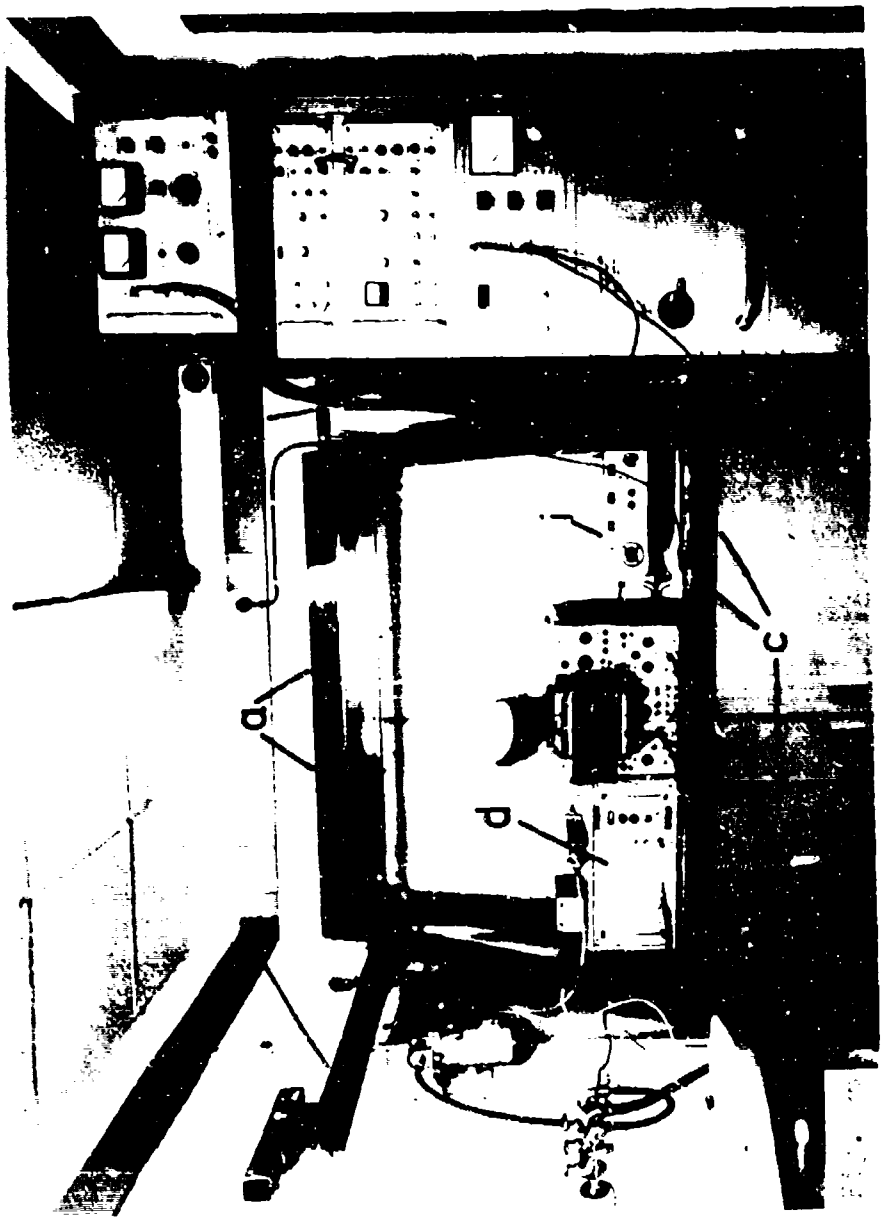

Fig. 27

SCEMATIC t^2-CONTROL UNIT

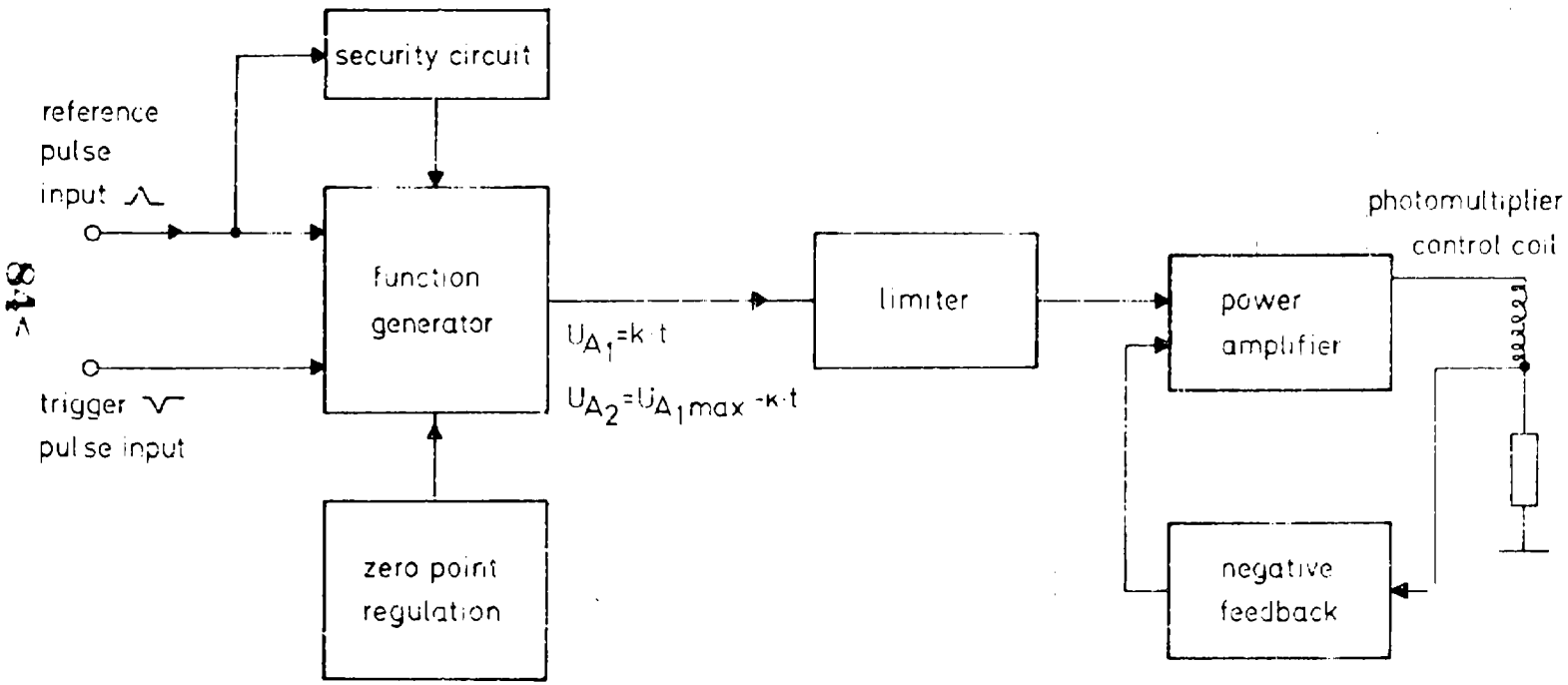

Fig. 28

SCHEMATIC, POWER SUPPLY

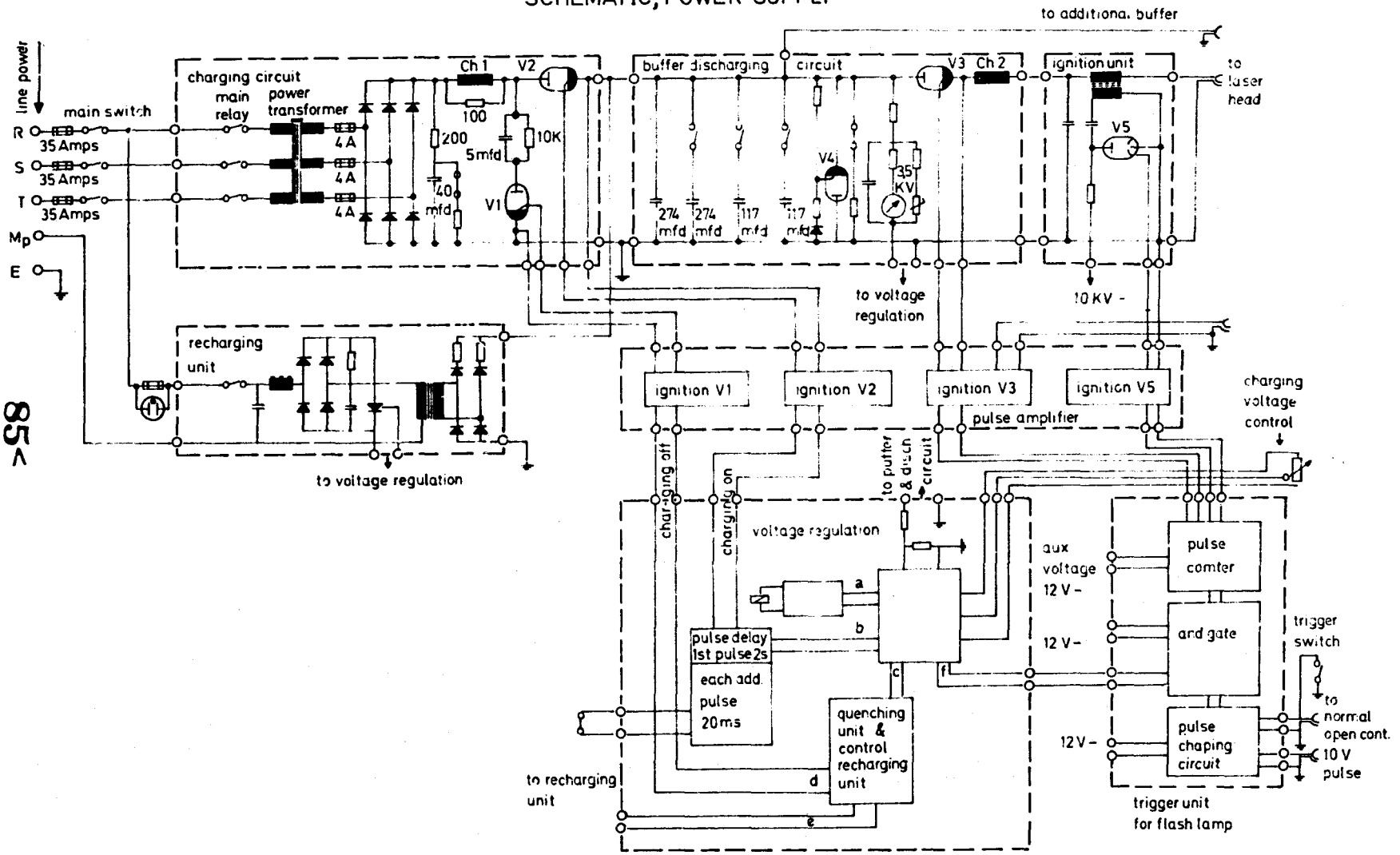

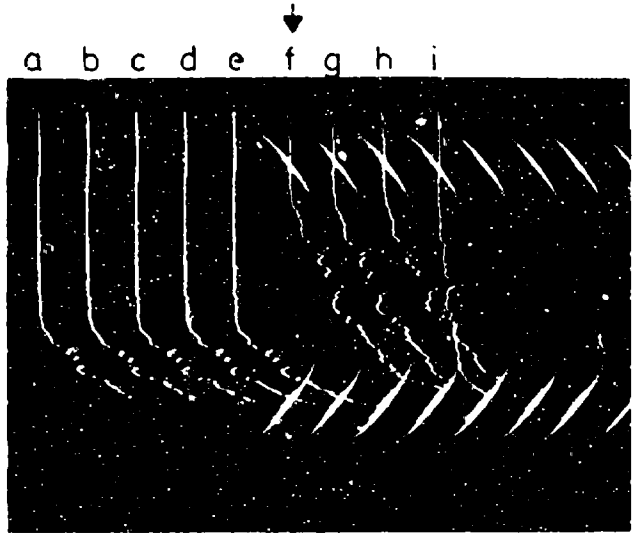

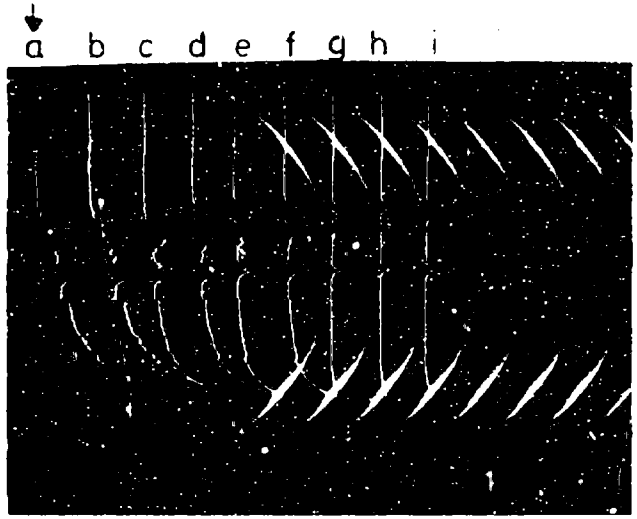

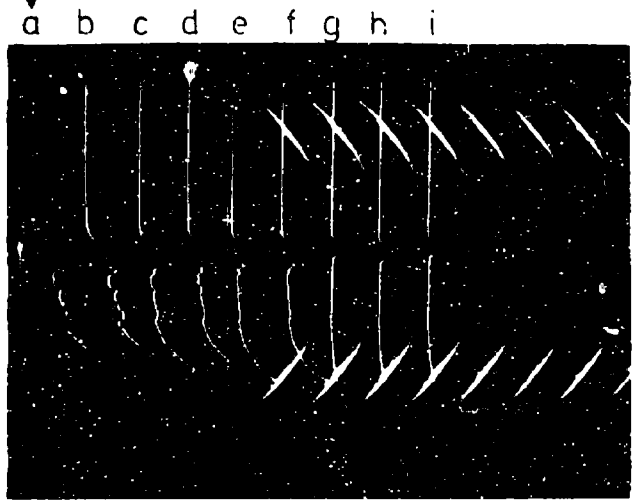

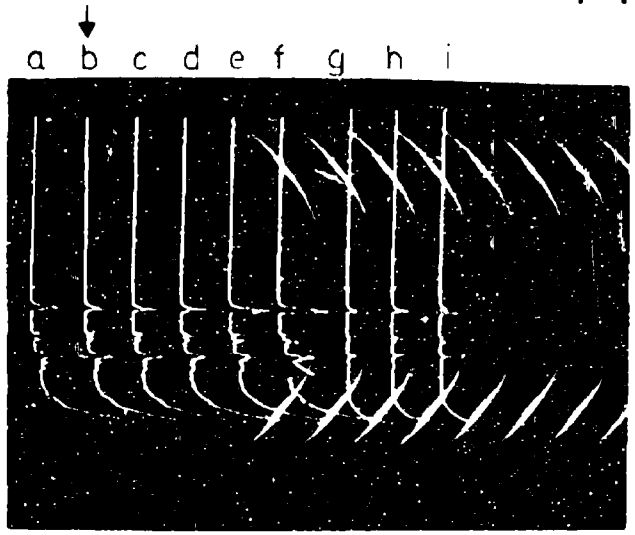

Fig.29

Fig. 30

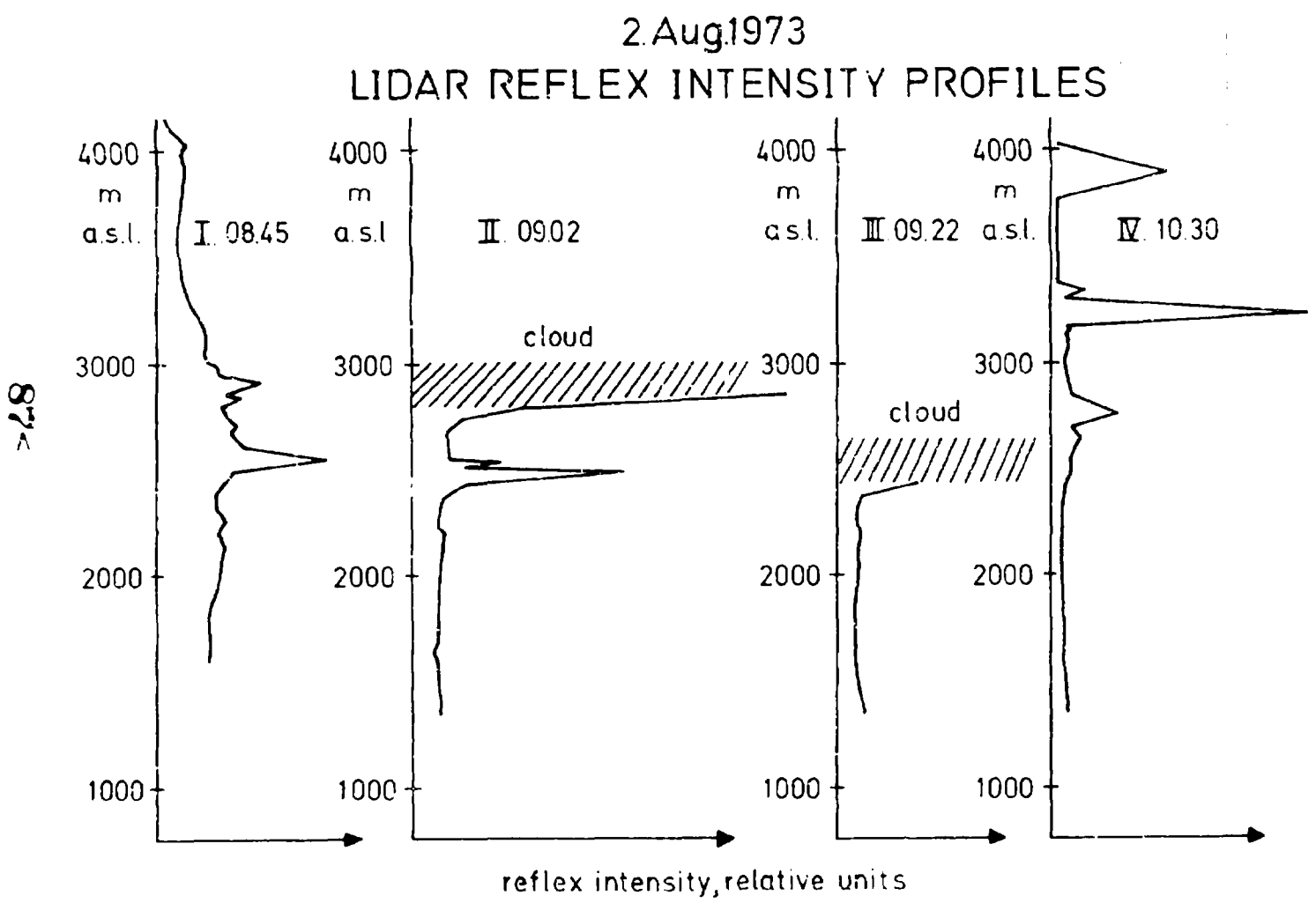
2. Aug. 1973
LIDAR REFLEX INTENSITY PROFILES
4000
m
a.s.l.
I. 08.45
II. 09.02
III. 09.22
IV. 10.30
cloud
cloud
3000
2000
1000
reflex intensity, relative units

Fig. 31

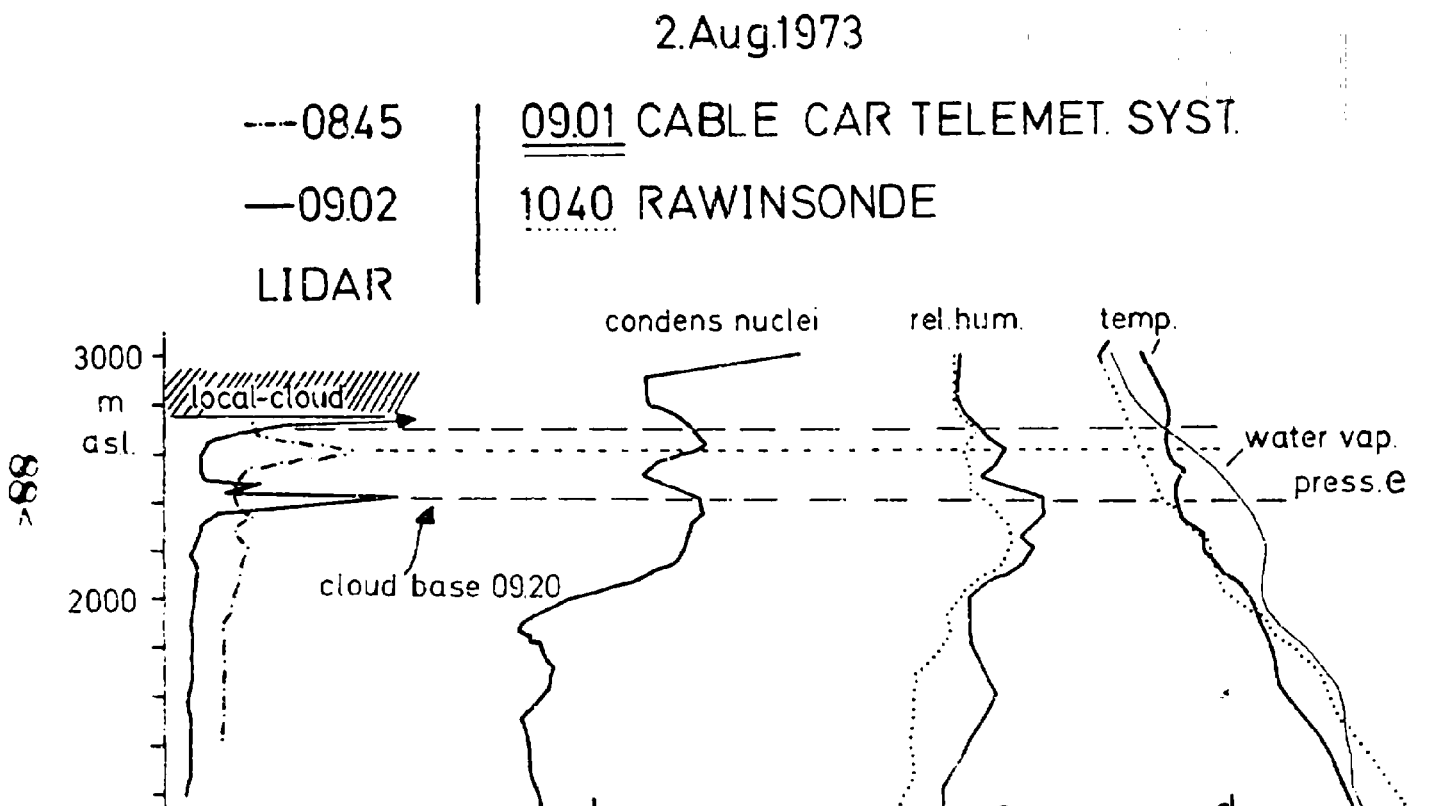
2.Aug.1973
---0845
09.01 CABLE CAR TELEMET. SYST.
—0902
1040 RAWINSONDE
LIDAR
condens nuclei
rel.hum.
temp.
3000
m
asl.
2000
1000
local-cloud
water vap.
press.e
cloud base 09.20
a
b
c
d
8
10
e
12
reflex intensity
rel.units
2
3
4
log(N/cm³)
40
60
100
% rel humidity
4
6
8
10
12
14
16
temp. °C

TABLE I

RaB in air; units $10^{-12}\mu C/cm^3$

Station Designations: Z Zugspitze 2964 m a.s.l.
W Wank 1780 m a.s.l.
G Garmisch-Partenkirchen 730 m a.s.l.

Measurement periods: a = 2150 - 0920, b = 0950 - 1220,
c = 1250 - 1620. (Central European Time)

Month: July 1972 ("No measurements" is denoted by: -)

	a			b			c		
	Z	W	G	Z	W	G	Z	W	G
1.	26,4	21	136	27,2	73	86	46,5	74	74
2.	-	-	218	-	-	63	-	-	-
3.	9,3	59	182	0,5	23	-	-	-	-
4.	1,7	51	-	28,9	54	-	37,2	67	-
5.	42,1	102	319	69,2	89	193	66,7	99	115
6.	34,2	61	300	23,0	65	211	10,1	60	143
7.	41,4	77	283	64,0	96	146	39,1	57	100
8.	26,3	89	263	59,9	96	147	68,2	104	140
9.	-	-	366	-	-	161	-	-	-
10.	73,5	-	145	1,6	7	28	-	6	46
11.	1,8	18	75	1,0	17	59	2,0	9	38
12.	4,3	10	201	2,1	12	206	4,9	7	132
13.	3,5	10	215	3,8	16	156	10,5	35	-
14.	13,2	80	208	26,7	89	155	-	62	73
15.	7,6	32	260	19,9	59	202	25,8	116	155
16.	-	-	346	-	-	211	-	-	-
17.	45,9	119	375	76,6	97	300	96,3	135	181
18.	47,3	-	367	90,6	57	235	65,9	87	157
19.	24,5	76	269	47,2	102	184	38,6	92	88
20.	52,5	78	292	74,4	138	178	68,6	86	-
21.	30,1	67	284	47,0	74	175	47,3	84	134
22.	41,3	134	463	47,8	125	111	42,6	94	122
23.	-	-	89	-	-	103	-	-	-
24.	29,5	95	316	66,4	109	173	55,3	98	146
25.	59,1	50	296	58,0	85	124	40,3	64	106
26.	7,1	41	290	19,9	57	104	25,9	47	104
27.	16,0	60	181	32,3	56	151	24,8	24	80
28.	8,5	17	157	16,1	10	144	12,4	19	122
29.	3,6	33	188	2,1	38	139	12,2	34	140
30.	-	-	217	-	-	106	-	-	-
31.	29,0	84	251	44,9	85	99	30,6	68	99

TABLE II

RaB in air; units $10^{-12}\mu C/cm^3$

Station Designations: Z Zugspitze 2964 m a.s.l.
W Wank 1780 m a.s.l.
G Garmisch-Partenkirchen 730 m a.s.l.

Measurement periods : a = 2150 - 0920, b = 0950 - 1220,
c = 1250 - 1620. (Central European Time)

Month: August 1972 ("No measurements" is denoted by: -)

	a			b			c		
	Z	W	G	Z	W	G	Z	W	G
1.	21,3	60	285	22,7	24	103	63,0	28	61
2.	24,4	59	228	22,5	32	63	34,9	22	66
3.	3,1	63	306	5,2	53	109	1,7	26	46
4.	0,8	4	94	0,7	13	50	5,0	21	46
5.	12,2	57	229	38,4	79	109	47,7	54	74
6.	-	-	299	-	-	128	-	-	-
7.	34,5	47	309	47,8	95	147	66,1	84	127
8.	101,1	208	465	121,3	183	228	131,1	138	204
9.	91,8	79	614	119,8	144	165	111,4	127	147
10.	49,9	153	480	99,3	160	207	111,9	133	177
11.	43,1	125	334	99,2	202	271	107,3	128	154
12.	110,8	204	432	131,7	191	366	146,3	194	302
13.	-	-	475	-	-	219	-	-	-
14.	33,7	98	311	67,6	95	175	78,5	91	280
15.	-	-	429	-	-	255	-	-	-
16.	18,7	43	219	9,4	51	147	11,7	60	133
17.	24,7	18	77	29,9	36	75	27,7	20	87
18.	7,4	58	234	0,0	26	112	1,6	17	55
19.	0,9	-	72	-	3	85	1,1	9	57
20.	-	-	153	-	-	78	-	-	-
21.	5,3	-	240	7,1	47	84	11,5	16	47
22.	3,2	15	101	1,6	8	59	1,4	5	58
23.	15,7	77	396	43,6	115	119	71,9	84	97
24.	33,1	-	349	15,9	103	117	32,7	82	115
25.	1,0	73	441	1,3	78	117	43,6	61	79
26.	1,3	81	388	17,0	81	196	75,0	87	115
27.	-	-	453	-	-	252	-	-	-
28.	36,1	106	811	62,6	117	509	66,4	189	188
29.	35,9	130	556	42,2	135	361	47,4	198	238
30.	84,4	129	347	74,0	191	259	93,5	97	200
31.	11,6	137	554	32,3	148	277	69,4	112	-

TABLE III

RaB in air; units $10^{-12}\mu C/cm^3$

Station Designations: Z Zugspitze 2964 m a.s.l.
W Wank 1780 m a.s.l.
G Garmisch-Partenkirchen 730 m a.s.l.

Measurement periods : a = 2150 - 0920, b = 0950 - 1220,
c = 1250 - 1620. (Central European Time)

Month: September 1972 ("No measurements" is denoted by: -)

	a			b			c		
	Z	W	G	Z	W	G	Z	W	G
1.	-	-	-	-	-	-	-	-	-
2.	-	-	-	-	-	-	-	-	-
3.	-	-	-	-	-	-	-	-	-
4.	-	-	-	-	-	-	-	-	-
5.	-	-	-	-	-	-	-	-	-
6.	55,6	130	690	96,0	98	287	96,2	215	295
7.	54,5	126	530	101,5	143	298	97,2	153	227
8.	91,5	120	590	78,1	109	295	77,5	99	145
9.	55,2	58	531	58,0	104	206	58,7	94	164
10.	-	-	456	-	-	159	-	-	-
11.	7,4	18	84	6,3	8	35	4,5	20	47
12.	11,9	33	459	21,8	27	81	22,8	56	64
13.	22,7	64	392	34,5	88	130	27,9	52	105
14.	37,9	202	406	84,4	121	337	78,4	109	209
15.	78,2	112	602	63,2	119	245	18,6	105	224
16.	-	12	152	10,7	86	131	10,1	51	164
17.	-	-	313	-	-	119	-	-	-
18.	30,3	83	337	37,8	79	146	37,9	53	99
19.	54,7	75	384	42,6	79	202	39,4	27	139
20.	74,2	123	421	76,7	104	230	86,7	148	193
21.	56,1	146	394	67,0	138	254	105,9	135	209
22.	5,1	135	416	1,3	113	316	12,6	148	312
23.	12,8	105	806	35,5	100	172	9,7	76	-
24.	-	-	125	-	-	50	-	-	-
25.	15,7	41	401	22,4	32	67	24,5	58	83
26.	17,3	97	383	51,0	131	271	81,2	84	132
27.	22,6	75	407	14,5	68	107	40,5	43	84
28.	2,9	51	386	19,8	58	200	38,9	37	78
29.	2,1	49	473	2,4	98	104	20,2	86	123
30.	3,3	62	351	10,5	121	-	56,5	160	186

TABLE IV

RaB in air; units $10^{-12}\mu C/cm^3$

Station Designations : Z Zugspitze 2964 m a.s.l.
W Wank 1780 m a.s.l.
G Garmisch-Partenkirchen 730 m a.s.l.

Measurement periods : a = 2150 - 0920, b = 0950 - 1220,
c = 1250 - 1620. (Central European Time)

Month: October 1972 ("No measurements" is denoted by: -)

	a			b			c		
	Z	W	G	Z	W	G	Z	W	G
1.	-	-	770	-	-	373	-	-	-
2.	-	160	821	-	187	452	-	245	304
3.	-	19	388	-	125	308	-	92	111
4.	-	43	-	-	93	301	-	124	126
5.	3,7	30	362	8,2	72	334	11,8	92	192
6.	15,2	49	443	24,2	126	406	48,1	186	385
7.	13,0	116	518	46,7	232	418	117,5	201	452
8.	-	-	695	-	-	306	-	-	-
9.	4,9	119	960	5,9	68	340	5,1	62	129
10.	22,8	66	364	24,6	116	229	51,0	95	194
11.	18,2	127	370	30,0	133	287	61,9	148	278
12.	22,3	88	389	30,5	88	452	42,6	113	503
13.	10,1	60	368	21,1	133	473	52,3	196	496
14.	3,6	208	521	3,6	130	337	9,4	206	256
15.	-	-	583	-	-	259	-	-	-
16.	4,4	33	512	5,7	-	534	18,3	130	333
17.	3,3	31	460	6,0	73	728	13,3	118	480
18.	2,2	37	731	10,7	85	301	29,2	81	110
19.	2,5	74	436	-	85	291	-	91	228
20.	6,3	71	638	6,0	88	476	4,0	82	336
21.	5,4	19	83	10,7	25	71	5,3	19	86
22.	-	-	64	-	-	127	-	-	-
23.	-	-	146	-	2	219	-	23	163
24.	1,2	29	231	0,8	35	214	11,1	69	140
25.	3,6	37	443	3,1	69	340	4,3	80	308
26.	6,3	28	386	5,3	51	239	8,9	88	285
27.	23,8	80	439	25,5	65	474	28,2	101	378
28.	10,7	64	389	-	7	107	4,2	8	58
29.	-	-	389	-	-	237	-	-	-
30.	11,1	47	436	4,1	56	448	3,4	104	332
31.	4,5	68	361	3,8	65	562	9,5	98	532

TABLE V

RaB in air; units $10^{-12}\mu C/cm^3$

Station Designations: Z Zugspitze 2964 m a.s.l.
W Wank 1780 m a.s.l.
G Garmisch-Partenkirchen 730 m a.s.l.

Measurement periods : a = 2150 - 0920, b = 0950 - 1220,
c = 1250 - 1620. (Central European Time)

Month: November 1972 ("No measurements" is denoted by: -)

	a			b			c		
	Z	W	G	Z	W	G	Z	W	G
1.	-	-	409	-	-	189	-	-	-
2.	0,7	34	395	0,2	109	256	0,3	93	200
3.	0,6	61	389	0,7	89	308	0,8	96	327
4.	7,6	22	347	8,8	26	382	31,5	79	233
5.	-	-	508	-	-	350	-	-	-
6.	1,0	31	436	3,5	75	306	2,6	92	195
7.	0,7	36	405	0,7	34	406	16,0	79	306
8.	5,3	19	374	3,4	86	344	7,8	199	217
9.	14,8	79	622	16,8	93	432	35,7	127	326
10.	13,9	50	463	23,9	58	340	56,8	112	233
11.	44,3	-	621	7,1	-	229	4,3	-	64
12.	-	-	90	-	-	55	-	-	-
13.	-	-	116	0,0	4	168	0,2	7	43
14.	0,4	12	235	-	12	219	0,4	11	253
15.	6,5	4	70	3,9	5	63	7,3	18	55
16.	1,8	25	210	5,8	19	192	10,6	102	198
17.	-	5	235	2,1	5	162	5,0	14	186
18.	1,5	-	73	5,4	-	40	5,1	-	60
19.	-	-	265	-	-	224	-	-	-
20.	29,0	-	296	31,6	72	253	22,2	48	347
21.	5,1	15	180	5,0	4	133	3,2	3	134
22.	0,5	10	354	0,0	7	404	0,7	2	345
23.	0,6	3	299	0,5	6	306	1,2	24	325
24.	2,3	13	63	6,2	16	109	6,1	21	106
25.	2,8	-	93	6,4	-	80	4,7	-	77
26.	-	-	306	-	-	216	-	-	-
27.	0,7	-	455	0,4	22	339	0,5	11	240
28.	1,1	3	284	0,7	21	291	4,2	29	306
29.	20,5	38	320	13,5	40	273	16,2	57	371
30.	25,7	66	412	28,0	55	362	38,4	59	334

TABLE VI

RaB in air; units $10^{-12}\mu C/cm^3$

Station Designations: Z Zugspitze 2964 m a.s.l.
W Wank 1780 m a.s.l.
G Garmisch-Partenkirchen 730 m a.s.l.

Measurement periods : a = 2150 - 0920, b = 0950 - 1220,
c = 1250 - 1620. (Central European Time)

Month: December 1972 ("No measurements" is denoted by:-)

	a			b			c		
	Z	W	G	Z	W	G	Z	W	G
1.	12,0	54	489	7,4	17	721	4,6	95	655
2.	22,3	-	220	24,8	-	263	31,7	-	410
3.	-	-	285	-	-	296	-	-	-
4.	39,9	-	507	26,0	86	328	39,7	63	363
5.	2,4	14	292	0,9	23	298	12,3	22	181
6.	1,8	27	318	-	13	251	1,3	36	271
7.	9,8	42	305	7,8	35	336	14,0	65	291
8.	56,5	104	-	44,4	178	515	72,6	147	497
9.	13,2	-	583	6,8	-	539	2,8	-	237
10.	-	-	320	-	-	232	-	-	-
11.	11,5	-	324	2,0	25	371	2,6	64	478
12.	7,7	22	245	8,1	29	284	12,7	69	450
13.	3,6	-	358	1,0	41	376	0,7	92	452
14.	2,7	32	343	0,1	20	373	3,5	49	588
15.	1,2	31	837	1,8	33	408	8,0	81	436
16.	-	-	280	0,8	-	371	1,8	-	490
17.	-	-	517	-	-	1113	-	-	-
18.	0,4	-	839	-	43	1061	0,3	59	992
19.	0,7	51	1159	9,9	61	1285	20,5	60	662
20.	2,5	59	841	1,2	71	753	2,3	91	564
21.	3,1	55	1029	1,9	47	877	2,2	128	943
22.	1,4	29	615	2,0	37	488	7,7	9	665
23.	3,4	17	214	8,0	27	250	10,0	24	352
24.	-	-	304	-	-	453	-	-	-
25.	-	-	320	-	-	746	-	-	-
26.	-	-	295	-	-	901	-	-	-
27.	26,3	57	391	21,5	37	344	27,6	45	169
28.	20,0	25	256	17,7	34	263	27,8	36	221
29.	12,0	46	345	13,8	57	560	77,9	95	431
30.	16,3	34	309	11,3	44	284	7,4	54	331
31.	-	-	313	-	-	497	-	-	-

TABLE VII

RaB in air; units 10^{-12} µC/cm^3

Station Desimnations: Z Zugspitze 2964 m a.s.l.
W Wank 1790 m a.s.l.
G Garmisch-Partenkirchen 730 m a.s.l.

Measurement periods : a = 2100 - 0900, B = 0900 - 1200,
c = 1200 - 1600. (Central European Time)

Month: January 1973 ("No measurements" is denoted by: -)

	a			b			c		
	Z1	W	G	Z	W	G	Z	W	G
1.	-	-	220	-	-	211	-	-	-
2.	11,2	15	261	14,9	12	476	18,4	14	558
3.	2,8	29	499	1,5	14	586	1,5	8	623
4.	0,5	43	237	-	27	396	-	25	330
5.	4,7	23	429	4,6	18	588	5,1	57	473
6.	-	-	1020	-	-	560	-	-	-
7.	-	-	-	-	-	-	-	-	-
8.	1,6	26	-	0,4	44	-	1,0	97	-
9.	1,1	72	-	0,3	79	-	0,7	106	-
10.	5,0	84	-	0,6	98	-	5,2	65	-
11.	0,5	51	628	1,1	37	755	1,9	66	735
12.	1,3	5	361	0,8	59	788	0,6	70	802
13.	1,3	-	1141	0,2	36	1015	5,6	71	903
14.	-	-	389	28,5	-	308	-	-	-
15.	28,5	81	-	27,4	79	470	77,4	52	613
16.	8,5	2	485	6,9	-	231	22,5	13	-
17.	26,0	65	374	27,3	75	492	25,8	96	417
18.	24,8	27	402	23,7	44	529	35,9	84	479
19.	29,5	70	1351	26,2	198	970	20,8	107	501
20.	60,9	125	796	12,7	119	877	32,8	88	655
21.	-	-	505	-	-	362	-	-	-
22.	45,9	14	869	30,0	7	326	64,3	17	193
23.	17,0	18	241	5,4	44	200	1,6	53	196
24.	9,5	1	370	6,3	9	297	13,9	65	413
25.	-	31	611	14,8	37	634	8,3	66	674
26.	2,8	67	405	1,6	58	370	2,9	97	302
27.	6,1	32	475	4,1	23	348	2,0	3	383
28.	-	-	-	-	-	-	-	-	-
29.	2,9	-	-	0,0	18	-	0,0	22	163
30.	0,1	10	409	-	13	452	3,4	16	392
31.	3,0	44	676	12,0	45	588	14,9	47	292

TABLE VIII

RaB in air; units $10^{-12}\mu C/cm^3$

Station Designations: Z Zugspitze 2964 m a.s.l.
W Wank 1780 m a.s.l.
G Garmisch-Partenkirchen 730 m a.s.l.

Measurement periods : a = 2150 - 0920, b = 0950 - 1250,
c = 1250 - 1620. (Central European Time)

Month: February 1973 ("No measurements" is denoted by: -)

	a			b			c		
	Z	W	G	Z	W	G	Z	W	G
1.	26,5	73	137	34,4	57	125	49,9	65	107
2.	48,4	100	141	42,5	74	186	26,3	58	159
3.	17,0	61	225	12,0	66	236	8,8	64	312
4.	-	-	581	-	-	567	-	-	-
5.	0,7	2	333	-	13	485	-	57	338
6.	0,5	48	342	10,6	59	392	19,5	51	333
7.	0,5	20	549	1,6	17	585	1,0	62	357
8.	14,0	28	652	12,2	48	312	17,1	103	158
9.	10,7	16	514	12,0	33	692	45,2	67	490
10.	13,9	37	590	6,0	19	270	5,0	14	90
11.	-	-	35	-	-	63	-	-	-
12.	-	15	103	2,3	12	94	1,5	21	153
13.	62,9	103	480	52,6	75	349	63,4	20	86
14.	3,9	13	226	6,3	15	211	32,5	22	190
15.	3,1	50	395	3,1	97	224	4,3	108	216
16.	5,0	96	890	3,8	98	695	1,9	150	300
17.	2,7	25	296	1,2	52	360	3,1	153	180
18.	-	-	147	-	-	24	-	-	-
19.	-	-	500	16,2	51	360	30,8	48	208
20.	-	76	477	6,6	65	295	4,9	90	129
21.	0,2	5	475	0,5	6	368	0,9	37	159
22.	5,1	10	264	0,2	8	177	2,7	11	134
23.	-	14	104	3,1	3	47	4,8	-	55
24.	1,5	-	112	3,3	-	53	-	-	48
25.	-	-	-	-	-	69	-	-	-
26.	2,3	18	388	2,7	30	127	2,9	13	58
27.	2,0	13	54	2,5	14	39	1,4	15	51
28.	0,9	14	443	0,5	14	162	-	35	96

TABLE IX

RaB in air; units $10^{-12}\mu C/cm^3$

Station Designations: Z Zugspitze 2964 m a.s.l.
W Wank 1780 m a.s.l.
G Garmisch-Partenkirchen 730 m a.s.l.

Measurement periods : a = 2150 - 0920, b = 0950 - 1220,
c = 1250 - 1620. (Central European Time)

Month: March 1973 ("No measurements" is denoted by: -)

	a			b			c		
	Z	W	G	Z	W	G	Z	W	G
1.	1,2	3	309	0,9	9	215	1,6	41	129
2.	32,9	48	354	19,2	74	394	27,9	84	210
3.	1,4	16	-	-	25	-	0,8	20	-
4.	-	-	-	-	-	-	-	-	-
5.	1,0	5	-	0,9	11	204	0,1	17	205
6.	6,7	12	290	10,4	10	319	35,8	22	108
7.	4,1	10	81	3,0	15	73	5,6	17	67
8.	7,5	7	65	0,01	10	51	2,7	9	49
9.	3,9	5	86	2,0	6	42	4,5	20	45
10.	-	24	326	-	35	99	-	21	50
11.	-	-	384	-	-	228	-	-	-
12.	2,0	17	436	-	66	389	-	42	146
13.	-	54	218	-	69	190	-	96	157
14.	-	43	178	-	50	149	-	47	126
15.	-	76	262	-	74	138	-	63	92
16.	-	60	409	-	90	191	-	61	75
17.	-	67	331	-	142	236	-	143	208
18.	-	-	466	-	-	273	-	-	-
19.	-	9	52	-	1	36	-	12	53
20.	-	26	335	-	84	177	-	76	154
21.	-	10	-	-	43	-	-	79	-
22.	-	25	-	-	38	-	-	55	-
23.	-	61	-	-	116	-	-	29	-
24.	-	-	-	-	19	-	-	85	-
25.	-	-	-	-	-	-	-	-	-
26.	-	92	-	-	108	-	-	77	-
27.	-	59	-	-	77	-	-	79	-
28.	57,7	89	-	54,9	95	-	85,7	89	-
29.	5,6	61	-	4,9	63	-	21,0	96	-
30.	29,7	78	-	29,9	88	-	84,8	100	-
31.	37,8	55	-	39,7	67	-	35,4	58	-

TABLE X

RaB in air; units $10^{-12}\mu C/cm^3$

Station Designations:
Z Zugspitze 2964 m a.s.l.
W Wank 1780 m a.s.l.
G Garmisch-Partenkirchen 730 m a.s.l.

Measurement periods : a = 2150 - 0920, b = 0950 - 1220, c = 1250 - 1620. (Central European Time)

Month: April 1973 ("No measurements" is denoted by: -)

	a			b			c		
	Z	W	G	Z	W	G	Z	W	G
1.	-	-	-	-	-	-	-	-	-
2.	13,3	30,	286	43,1	43	154	80,9	-	176
3.	3,3	11	20	3,6	8	28	3,3	6	27
4.	-	8	28	9,1	7	37	2,0	11	46
5.	1,4	10	264	0,4	23	158	-	38	155
6.	4,0	39	313	8,4	57	121	26,6	46	82
7.	-	13	55	25,3	17	46	18,2	29	66
8.	-	-	95	-	-	63	-	-	-
9.	57,9	56	139	43,1	53	137	56,1	51	128
10.	5,1	75	221	54,3	58	250	41,3	41	139
11.	-	38	103	19,0	28	51	23,9	19	54
12.	-	18	-	23,8	6	16	8,1	9	30
13.	-	15	-	8,5	13	38	5,9	10	32
14.	-	-	230	15,0	14	46	12,5	16	46
15.	-	-	220	-	-	53	-	-	-
16.	5,6	53	-	13,9	69	166	21,9	28	91
17.	4,0	56	332	8,7	38	52	9,3	33	-
18.	-	9	-	4,4	11	-	7,4	8	-
19.	-	9	-	-	3	-	4,9	13	39
20.	-	-	-	-	-	37	-	-	-
21.	-	16	47	-	17	34	14,8	22	41
22.	-	-	265	-	-	139	-	-	-
23.	-	-	309	-	-	194	-	-	-
24.	30,0	66	-	26,2	75	-	47,6	75	156
25.	6,0	24	319	15,6	59	169	17,2	55	141
26.	13,8	34	271	19,6	48	142	48,9	41	87
27.	42,5	53	197	54,5	60	139	44,9	38	-
28.	46,1	88	-	72,6	60	174	80,7	55	151
29.	-	-	247	-	-	110	-	-	-
30.	15,8	72	198	31,9	73	151	79,6	66	147

TABLE XI

RaB in air; units $10^{-12}\mu C/cm^3$

Station Designations:
Z Zugspitze 2964 m a.s.l.
W Wank 1780 m a.s.l.
G Garmisch-Partenkirchen 730 m a.s.l.

Measurement periods : a = 2150 - 0920, b = 0950 - 1220,
c = 1250 - 1620. (Central European Time)

Month: May 1973 ("No measurements" is denoted by: -)

	a			b			c		
	Z	W	G	Z	W	G	Z	W	G
1.	-	-	237	-	-	139	-	-	-
2.	33,3	82	330	45,7	68	-	76,9	57	-
3.	42,1	64	-	60,1	-	-	76,7	-	-
4.	21,5	-	254	25,3	-	-	70,1	-	198
5.	76,7	-	268	25,9	-	131	31,9	-	116
6.	-	-	-	-	-	-	-	-	-
7.	16,2	-	142	24,4	-	102	27,1	-	-
8.	5,7	3	-	8,8	27	61	19,0	18	27
9.	5,4	6	132	8,4	13	145	12,5	21	56
10.	5,8	-	230	4,8	-	99	6,6	-	89
11.	-	-	103	-	-	-	-	-	76
12.	11,0	-	122	16,9	-	55	39,2	-	50
13.	-	-	170	-	-	85	-	-	-
14.	36,0	42	268	50,8	47	126	42,6	44	95
15.	40,2	50	221	44,1	70	209	45,6	52	115
16.	41,5	-	180	49,4	30	184	19,1	57	119
17.	75,9	91	311	21,2	87	100	41,7	83	117
18.	25,6	98	402	29,7	86	278	111,9	96	195
19.	15,5	77	280	25,7	51	188	79,5	52	246
20.	-	-	119	-	-	127	-	-	-
21.	41,3	70	197	52,6	48	113	38,7	29	43
22.	15,9	44	167	35,3	30	90	65,7	39	78
23.	12,3	18	74	20,1	16	52	31,0	19	48
24.	-	25	219	27,7	34	99	22,5	23	65
25.	37,3	16	133	32,8	28	67	32,2	23	61
26.	6,1	74	216	22,8	57	106	44,3	52	79
27.	-	-	243	-	-	-	-	-	-
28.	41,9	69	326	33,5	96	243	89,3	54	144
29.	90,9	96	379	89,5	83	174	37,5	68	-
30.	55,9	20	139	75,4	94	107	90,1	70	-
31.	-	-	-	-	-	-	-	-	-

TABLE XII

RaB in air; units $10^{-12}\mu C/cm^3$

Station Designations:
Z Zugspitze 2964 m a.s.l.
W Wank 1780 m a.s.l.
G Garmisch-Partenkirchen 730 m a.s.l.

Measurement periods : a = 2150 - 0920, b = 0950 - 1220,
c = 1250 - 1620. (Central European Time)

Month: June 1973 ("No measurements" is denoted by: -)

	a			b			c		
	Z	W	G	Z	W	G	Z	W	G
1.	60,0	326	-	111,6	125	-	133,3	88	222
2.	66,4	134	306	52,0	35	119	62,1	7	79
3.	-	-	143	-	-	98	-	-	-
4.	31,5	97	261	48,7	102	199	76,4	76	108
5.	75,5	22	320	80,5	169	312	78,9	143	182
6.	40,8	135	-	49,6	135	-	14,7	64	215
7.	40,9	56	186	31,0	77	158	23,4	28	104
8.	30,9	42	285	32,2	65	266	34,2	46	123
9.	6,7	50	137	10,3	19	158	16,2	-	82
10.	-	-	217	-	-	100	-	-	-
11.	-	-	278	-	-	121	-	-	-
12.	12,4	-	301	50,7	71	274	91,4	129	160
13.	43,8	-	270	75,1	138	162	64,0	60	136
14.	16,7	33	420	21,6	63	205	20,3	2	68
15.	1,2	46	165	1,	49	87	12,7	22	59
16.	0,8	33	266	21,6	68	216	45,7	61	115
17.	-	-	280	-	-	99	-	-	-
18.	13,6	27	92	4,3	7	65	14,3	8	116
19.	17,7	45	210	27,9	34	97	37,8	28	73
20.	55,2	63	368	80,4	75	205	76,0	58	162
21.	-	-	41	-	-	59	-	-	-
22.	29,4	44	162	27,0	47	164	4,0	21	165
23.	54,5	182	350	58,7	118	242	24,7	36	139
24.	-	-	182	-	-	177	-	-	-
25.	13.6	45	217	16,6	79	256	26,1	62	99
26.	59,3	99	249	72,9	67	215	94,1	102	131
27.	32,8	153	222	56,4	126	231	91,0	131	198
28.	75,0	193	453	46,7	183	307	78,9	120	185
29.	15,0	29	145	19,8	20	122	24,6	10	59
30.	16,9	-	-	32,9	59	-	49,5	27	-